Phagocyte dynamics in a highly regenerative urochordate: Insights into development and host defense

Robert J Lauzon, Christina Brown, Louie Kerr, Stefano Tiozzo

Developmental Biology ▮ (▮▮▮▮) ▮▮▮–▮▮▮

Contents lists available at SciVerse ScienceDirect

Developmental Biology

journal homepage: www.elsevier.com/locate/developmentalbiology

Phagocyte dynamics in a highly regenerative urochordate: Insights into development and host defense

Robert J. Lauzon [a,*], Christina Brown [a], Louie Kerr [b], Stefano Tiozzo [c]

[a] Department of Biological Sciences, Union College, Science and Engineering Center, Schenectady, NY 12308, United States
[b] Marine Biological Laboratory, Woods Hole, MA 02543, United States
[c] Université Pierre et Marie Curie, Univ Paris 06UMR7009 CNRS, Observatoire Oceanologique, 06230 Villefranche-sur-mer, France

ARTICLE INFO

Article history:
Received 4 September 2012
Received in revised form
31 October 2012
Accepted 9 November 2012

Keywords:
Ascidian
Botryllus
Parabiosis
Phagocytosis
Regeneration
Homeostasis

ABSTRACT

Phagocytosis is a cellular process by which particles and foreign bodies are engulfed and degraded by specialized cells. It is functionally involved in nutrient acquisition and represents a fundamental mechanism used to remove pathogens and cellular debris. In the marine invertebrate chordate *Botryllus schlosseri*, cell corpse engulfment by phagocytic cells is the recurrent mechanism of programmed cell clearance and a critical process for the successful execution of asexual regeneration and colony homeostasis. In the present study, we have utilized a naturally occurring process of vascular parabiosis coupled with intravascular microinjection of fluorescent bioparticles and liposomes as tools to investigate the dynamics of phagocyte behavior in real-time during cyclical body regeneration. Our findings indicate that *B. schlosseri* harbors two major populations of post-mitotic phagocytes, which display distinct phagocytic specificity and homing patterns: a static population that lines the circulatory system epithelia, and a mobile population that continuously recirculates throughout the colony and exhibits a characteristic homing pattern within mesenchymal niches called ventral islands (VI). We observed that a significant proportion of ventral island phagocytes (VIP) die and are engulfed by other VIP following takeover. Selective impairment of VIP activity curtailed zooid resorption and asexual development. Together, these findings strongly suggest that ventral islands are sites of phagocyte homing and turnover. As botryllid ascidians represent invertebrate chordates capable of whole body regeneration in a non-embryonic scenario, we discuss the pivotal role that phagocytosis plays in homeostasis, tissue renewal and host defense.

Introduction

Cells that engulf and digest other cells in order to feed or eliminate foreign materials are generally referred to as phagocytes. In addition to their ability to "eat", phagocytic cells are mobile by means of pseudopodia and can generally disperse throughout the organism or within certain internal compartments (Stuart and Ezekowitz, 2005; Hume, 2006). Moreover, phagocytes are endowed with other specialized properties, which generally include a remarkable biosynthetic capacity combined with extraordinarily diverse patterns of gene expression (Delves et al., 2006). Phagocytic cells can be found across widely differing multicellular taxa: in animals without a digestive tract, phagocytes function primarily as nutritive cells, whereas in animals with a gut, these cells have acquired novel functions that are geared toward the maintenance of organismal integrity, such as host defense and the regulation of cellular turnover (Nakanishi et al., 2011). Since the first considerations of Metchnikoff, while developing his "phagocytosis theory", it has become clear that phagocytes not only play a role in immune defense but also in development and tissue homeostasis, via removal of cells that have become unwanted (Tauber, 2003; Nakanishi et al., 2011). The physiological process by which unnecessary or dangerous cells are selectively and safely eliminated occurs via apoptosis (Jacobson et al., 1997; Elliot and Ravichandran, 2010). Apoptotic cells are efficiently recognized, engulfed and digested by phagocytic cells in order to prevent necrotic cell lysis and the release of pro-inflammatory molecules. This homeostatic process, called programmed cell clearance (PCC), is essential in the maintenance of organismal health and integrity, as defects in recognition, engulfment or other steps in cell corpse clearance have been functionally linked with specific disease states in humans, including atherosclerosis, neuropathies, tumorigenesis and autoimmunity (Henson et al., 2001; Erwig and Henson, 2007; Schulze et al., 2008; Elliot and Ravichandran, 2010). Thus, phagocyte-mediated PCC allows apoptosis to be kept immunologically silent, while

* Corresponding author. Fax: +1 518 388 6429.
E-mail address: lauzonr@union.edu (R.J. Lauzon).

0012-1606/$ - see front matter © 2012 Elsevier Inc. All rights reserved.
http://dx.doi.org/10.1016/j.ydbio.2012.11.006

promoting tissue renewal and remodeling. PCC is not restricted to mammals but is also widespread in multicellular animals, and has been documented in teleosts, insects and nematodes (Fadeel, 2003; Fadeel et al., 2010). Most of the genes involved in the clearance of apoptotic cells are the same ones responsible for recognition, engulfment and intracellular digestion by phagocytes (Reddien and Horvitz, 2004; Stuart and Ezekowitz, 2005). Furthermore, these genes have counterparts in nematodes, flies, mice and humans, suggesting a phylogenetic conservation of the genetic program underlying PCC (Lettre and Hengartner, 2006; Kinchen and Ravichandran, 2007, 2010).

Ascidians (sub-phylum: Tunicata, phylum: Chordata) are closely related to vertebrates and possess a unique developmental plasticity (Lemaire, 2009). Colonial ascidians can generate and/or regenerate their entire body on a weekly basis throughout a wide diversity of developmental pathways (Kawamura et al., 2008; Tiozzo et al., 2008a; Tiozzo and Tomaso, 2009; Kürn et al., 2011). We study *B. schlosseri*, a colonial ascidian that grows via continuous cycles of asexual budding (called blastogenesis) that resume with a massive wave of apoptosis and phagocytosis. Each *B. schlosseri* colony consists of genetically identical units, named zooids, arranged into star-shaped systems. Each zooid propagates asexually by producing one or more primary buds as outgrowths of its lateral wall (Berrill, 1941; Milkman, 1967; Sabbadin, 1969, 1979; Izzard, 1973; Burighel and Cloney, 1997; Manni et al., 2007). The adult zooids and their buds are embedded in a transparent, gelatinous extracellular matrix, called tunic, and inter-connected by extracorporeal blood vessels that extend into protrusions called ampullae at the colony's periphery (Milkman, 1967; Sabbadin, 1969; Kürn et al., 2011). Moreover, blood flows within each adult zooid through a network of sinuses and lacunae (Burighel and Brunetti, 1971; Mukai et al., 1978; Tiozzo et al., 2008b). From its first appearance, each bud takes two blastogenetic cycles or approximately 10 days (at 21 °C) to reach maturity, then functionally replaces the parental zooid, following a massive wave of apoptosis in a process called takeover (Burighel and Schiavinato, 1984; Lauzon et al., 1992, 1993, 2002; Tiozzo et al., 2006; Ballarin et al., 2008). During takeover, up to half of the colony mass dies followed by programmed cell clearance via phagocytic cells that circulate in the sinuses and lacunae of adult zooids and buds, and in the extracorporeal vascular system (Burighel and Schiavinato, 1984; Lauzon et al., 1993; Voskoboynik et al., 2004; Lauzon et al., 2007). Zooid resorption is completed in 24–36 h (Lauzon et al., 2002; Manni et al., 2007; Kürn et al., 2011). Thus, during blastogenesis, botryllid ascidians use apoptosis and PCC as developmental tools to maintain colony homeostasis (Lauzon et al., 2002, 2007). We have previously proposed that a phagocytosis-dependent, macromolecular recycling mechanism is intrinsic to the reconstitution of a functional asexual generation with each round of blastogenesis (Lauzon et al., 2007; Kürn et al., 2011). Ballarin and colleagues have described two distinct phagocytic cell populations from blood in *B. schlosseri* colonies, based on morphological and histoenzymatic properties: the hyaline amebocytes and macrophage-like cells (Ballarin et al., 1993, 1994; Ballarin and Cima, 2005). However, the hematopoietic origin and spatial distribution of phagocytes, and in vivo behavior of these cells throughout blastogenesis remains unknown.

In this study, *B. schlosseri* was used as a chordate model to investigate the dynamic behavior and homing properties of phagocytic cells during the entire asexual development of the colony. Fluorescent bioparticle microinjection was used in combination with epifluorescence and confocal microscopy imaging to selectively target and visualize phagocytic cells in real time. We determined their spatial distribution patterns in situ and analyzed phagocyte function via chemical inhibition of phagocytic activity. Our results revealed the presence of two different populations of phagocytes with distinct homing behaviors and roles in organismal regeneration and defense.

Methods

Animal collection and maintenance

B. schlosseri colonies were collected in the Eel Pond at the Marine Biological Laboratory (Woods Hole, MA) during the summer months between 2004 and 2009 and maintained in flowing seawater tables between 20 and 22 °C. Clonal replicates were generated from multisystem colonies, staged according to Sabbadin (1955, 1956). Microsurgeries (complete and hemibudectomies) were carried out as previously described (Lauzon et al., 2002, 2007). Vascular parabiosis was performed as previously described (Scofield et al., 1982; De Tomaso et al., 2005).

Intra-ampullar microinjection and real-time imaging

Microinjection in *B. schlosseri* colonies was carried out as previously described (Laird et al., 2005; Tiozzo et al., 2008b) using a CellTram Vario hydraulic microinjector (Brinkmann–Eppendorf, Westbury, NY) and Leitz micromanipulator (Leitz, Germany). Lyophylized Alexafluor-conjugated, *Escherichia coli*, *Staphylococcus aureus* and *Saccharomyces cerevisiae* bioparticles, and pHrodo-conjugated *E. coli* bioparticles were reconstituted in 100 μl of phosphate buffered saline (PBS), according to the manufacturer's specifications (Invitrogen, Carlsbad, CA) and stored at 4 °C until needed. Prior to each experiment, 1 μl of the bioparticle stock was diluted with 3 μl of PBS and back-loaded in a glass needle with 2 μl volumes at a time. Alexafluor 594-conjugated, carboxylated microspheres (1 μm diameter) (Invitrogen) were diluted 1:1 in PBS, whereas India Ink was diluted 1:2 in PBS prior to microinjection, respectively. Intravascular microinjection was carried out via puncture of a healthy ampulla proximal to the marginal vessel that surrounds a *B. schlosseri* colony. 1 μl was the standard volume microinjected in small, one- (or two) system colonies comprised of 6–10 zooids. Successful microinjection was determined by visualizing fluorescent dye incorporation in the colonial vasculature and blood sinuses/lacunae of adult zooids and buds under epifluorescence stereomicroscope using an Zeiss SV8 stereomicroscope equipped with a Quad stereo fluorescence illuminator (Kramer Scientific LLC, Amesbury, MA) and an Exfo X-cite mercury-halide light source (Lumen Dynamics Group Inc., Mississauga, ON, Canada). Confocal imaging was carried on an LSM 510 Meta confocal laser-scanning microscope (Carl Zeiss Inc., Thornwood, NY) equipped with a krypton–argon laser and helium–neon lasers, using 20× and 40× planachromat water immersion objectives (Carl Zeiss Inc.).

Fluorescent liposome preparation

Clodronate (dichloromethylene diphosphonate) was purchased from Sigma-Aldrich (St. Louis, Missouri). Fluorescent PBS and clodronate liposomes were prepared according to the general method described by van Rooijen (1989), van Rooijen and Sanders (1994), van Rooijen and van Kesteren-Hendrikx (2003). For cholestryl BODIPY liposomes, 3.4 mg of phosphatidylcholine, 0.45 mg of unlabeled cholesterol (Avanti Polar Lipids, Alabaster, Alabama) and 50 μg of cholesteryl BODIPY 576/589 C11 (Invitrogen, Carlsbad, CA) were dissolved in 1 ml of chloroform (Sigma-Aldrich) within the confines of a round bottom flask. For BODIPY phosphocholine 503/512, 3.70 mg of unlabeled phosphatidylcholine (Avanti Polar Lipids), 50 μg of β-BODIPY FL C_{12}-HPC

Please cite this article as: Lauzon, R.J., et al., Phagocyte dynamics in a highly regenerative urochordate: Insights into development and host defense. Dev. Biol. (2012), http://dx.doi.org/10.1016/j.ydbio.2012.11.006

(Invitrogen) and 0.55 mg of unlabeled cholesterol were dissolved in 1 ml of chloroform. The chloroform was removed by low vacuum in a rotary evaporator at room temperature and the lipid film was dried under nitrogen gas for 5 min. For PBS liposomes, the lipid film was dispersed by adding 500 μl of PBS by gentle rotation for 30 min at room temperature. For clodronate liposome preparations, 500 μl of a 0.7 M clodronate solution (pH=7.1) was added to the lipid film, followed by gentle rotation for 15 min. Both suspensions were further maintained for 2 h at room temperature without rotation, and subsequently sonicated for 5 min. The suspensions were incubated overnight at 4 °C to allow swelling of liposomes, and then centrifuged at 22,000*g* for 60 min at 4 °C. The PBS liposome pellet was washed three times in PBS, and resuspended in 500 μl of PBS. For clodronate liposomes, the white band that formed at the top of the suspension following centrifugation was carefully collected and washed four times in PBS and subsequently resuspended in 500 μl of PBS. Both PBS and clodronate liposomes were stored at 4 °C.

Histology

Small, developmentally-staged colonies consisting of one or two systems of zooids were anaesthetized in MS-222 (Tricaine) (Sigma-Aldrich, St. Louis, MO) for five minutes, and fixed in 4% paraformaldehyde/PBS (pH=7.4) for two hours at 4 °C. They were subsequently washed four times in PBS (pH=7.4) for 15 min each and subsequently infiltrated in molten polyester wax (Electron Microscopy Sciences) for 2 h at 42 °C. The molten wax was replaced once and colonies were incubated overnight at 42 °C to ensure complete specimen infiltration, and subsequently embedded in square microtome embedding molds (VWR Scientific).

Six micron, serial tissue sections were cut from single system colonies using an LKB Bromma 2218 Historange Microtome (Uppsala, Sweden) and adhered onto Fisherbrand SuperFrost Plus glass microscope slides (ThermoFisher scientific, Waltham, MA). Polyester wax removal and tissue section rehydration was performed using a graded ethanol series, and stained with hematoxylin and eosin according to standard protocols.

Whole mount immunohistochemistry

Single system colonies containing 6–10 adult zooids were microinjected with 1 μl of pHrhodo *E. coli* bioparticles (previously reconstituted in 100 μl of PBS, according to the manufacturer's specifications) (Invitrogen). Twenty-four hours later, individual colonies were anaesthetized in MS-222 (Tricaine) for five minutes, subsequently fixed in 4% paraformaldehyde/PBS for thirty minutes and washed four times in PBS (15 min each) on a rotating shaker. This was followed by fixation in cold acetone (−20 °C) for one minute and three washes in PBS. Samples were permeabilized overnight in a solution consisting of 0.1% sodium citrate and 0.5% triton x-100 in PBS (pH=7.4) on a rotating shaker at room temperature, and subsequently incubated for two hours in blocking buffer (BB: 5% Normal Goat Serum, 0.5% Triton-X 100 diluted in PBS) at room temperature. Specimens were then incubated with a Phospho-Histone H3 rabbit polyclonal antibody (PHH3: Cell Signaling Technology, Danvers, MA) diluted 1:100 in 0.5% triton x-100/PBS for 48 h at 4 °C. All samples were washed in PBS and subsequently incubated overnight at 4 °C with an AlexaFluor 594-conjugated goat anti-rabbit IgG (Invitrogen) previously diluted 1:100 in 0.5% triton x-100/PBS. Specimens were washed four times in 0.5% triton x-100/PBS in the dark for 30 min each to remove unbound secondary antibody, and subsequently counterstained with DAPI (1 μg/ml in PBS) (Sigma-Aldrich, St-Louis, MO) for five minutes at room temperature. Specimens were washed twice for 10 min each in PBS, allowed to air dry and mounted in Fluoro-Gel anti-fading reagent (Electron Microscopy Sciences). Specimens were imaged on an LSM 510 Meta confocal microscope (Carl Zeiss Inc.), as described above.

Immuno-blotting

B. schlosseri colonies were developmentally staged and flash-frozen stored at −70 °C until needed. Colonies consisting of six to eight systems at stage 9/8/2 of blastogenesis were ground into a fine powder in liquid nitrogen by using a mortar and pestle, and processed as previously described (Lauzon et al., 1993). Lysates derived from approximately $20–30 \times 10^6$ cultured mouse HT-2 lymphocytes grown in the presence of interleukin 2 were used as a positive control. Protein concentrations were determined using the Bradford Assay (Bradford, 1976). 40 μg and 20 μg of protein from *B. schlosseri* and HT-2 lysates were used, respectively. SDS-PAGE, electroblotting and antibody incubations were carried out as previously described (Lauzon et al., 1993). Nitrocellulose membranes were incubated overnight at 4 °C with a rabbit polyclonal, anti phospho-histone H3 (Ser10) IgG antibody (Cell Signaling Technology, Danvers, MA) diluted 1:1000 in 10 ml of antibody buffer (5% non-fat dry milk, 10 mM Tris–HCl ph=7.5, 100 mM NaCl, 0.1% Tween 20). Following several washes (10 mM Tris pH=7.5, 100 mM NaCl, 0.1% Tween 20), the membranes were incubated with a secondary, alkaline phosphatase conjugated goat anti-rabbit IgG antibody (Jackson Immunoresearch Laboratory, Bar Harbor, ME) diluted 1:1000 in antibody buffer for 90 min and stained using NBT/BCIP (Roche Diagnostics, Mannheim, Germany), as previously described (Lauzon et al., 1993).

Transmission electron microscopy (TEM)

Small, single system colonies were developmentally-staged and fixed in a solution of 1% glutaraldehyde/0.2 M sodium cacodylate buffer (pH=7.4) (Electron Microscopy Sciences, Hatfield, PA) for three hours at room temperature followed by three, twenty minute washes in the same buffer. Samples were subsequently post-fixed in 1% osmium tetroxide/sodium cacodylate buffer (Electron Microscopy Sciences) for one hour on ice and washed three times in the same buffer for 10 min each. The specimens were dehydrated on ice in a graded ethanol series and finally, three times (fifteen minutes each) in propylene oxide on a rotating shaker. Specimens were subsequently infiltrated and embedded in Araldite 502/Embed-812 embedding media (Electron Microscopy Sciences) according to the manufacturer's specifications. Semithin and ultrathin sections were cut and placed onto formvar-coated, 100-mesh nickel grids (Electron Microscopy Sciences), and stained with 2% aqueous uranyl acetate and 1% lead citrate. Samples were then examined with a Zeiss 10CA transmission electron microscope (Carl Zeiss Inc., Thornwood, NY) and images were captured with an 1Kx1K AMT digital camera (Advanced Microscopy Techniques, Corp., Woburn, MA).

Results

Identification of two populations of phagocytes during blastogenetic development

In order to determine the spatial distribution of phagocytic cell populations during cyclic blastogenesis in *B. schlosseri*, we developed an experimental strategy to track their dynamics and homing patterns within living colonies. We hypothesized that, as bacteria (bioparticles) represent natural substrates for phagocytic cells, their engulfment could be used as a tool for phagocyte localization. We thus utilized microinjection of bioparticles coupled to the

Please cite this article as: Lauzon, R.J., et al., Phagocyte dynamics in a highly regenerative urochordate: Insights into development and host defense. Dev. Biol. (2012), http://dx.doi.org/10.1016/j.ydbio.2012.11.006

photostable Alexafluor dyes, and subsequently followed ingested fluorescence to monitor phagocyte populations in real time. Alexafluor-conjugated *E. coli* bioparticles were initially administered in the colonial vasculature via intra-ampullar microinjection (see Methods). Upon microinjection of Alexafluor 488- or 594-conjugated bioparticles, the marginal vessel that lies at the periphery of the colony and other extra-corporeal blood vessels became fluorescently labeled (Suppl. Fig. 1A). Within two minutes following microinjection, fluorescence was distributed throughout the extra-corporeal vasculature as well as the sinuses/lacunae within adult zooids and developing buds (Suppl. Fig. 1B). Eight hours following microinjection, a punctate fluorescence pattern was observed within adult zooids or pre-functional zooids (Fig. 1A). Within twenty-four hours, the fluorescent bioparticles were distributed within phagocytic cells that had formed discrete islands localized in the ventral mesenchyme of adult zooids. The zooid ventral islands (VI) were distributed bilaterally to the endostyle, along the zooid's antero-posterior axis (Fig. 1B and C). VI cellularity was most pronounced in the early stages of blastogenesis, between 9/7/1+ and 9/8/2 (Fig. 1C and D), after which cellularity consistently decreased within the VI: this included stages 9/8/3 (data not shown), 9/8/4 (Fig. 1E) and 9/8/5 (Fig. 1F). During these blastogenetic stages, fluorescent staining was consistently observed within the digestive tract (stomach and intestine) of adult zooids, possibly revealing an excretory mechanism for bioparticles and/or effete phagocytes (Fig. 1E and F). Moreover, phagocytes were also observed within sinuses and lacunae of adult zooids and throughout the colonial vasculature (described below and in Fig. 2). During the takeover phase of blastogenesis, the VI dissociated, and the resorbing adult zooids were extensively labeled with phagocytic cells (Fig.1A and G). As takeover proceeded, VI gradually re-appeared in the pre-functional zooid generation (Fig. 1G and H). At the onset of a new blastogenetic cycle, VI were once again visible in the filter-feeding, adult zooids (Fig. 1H). Similar observations were recorded when individual zooids were repeatedly monitored throughout blastogenesis. Phagocyte density within the VI was greatest in stages 9/7/1+ and 9/8/2–3 but

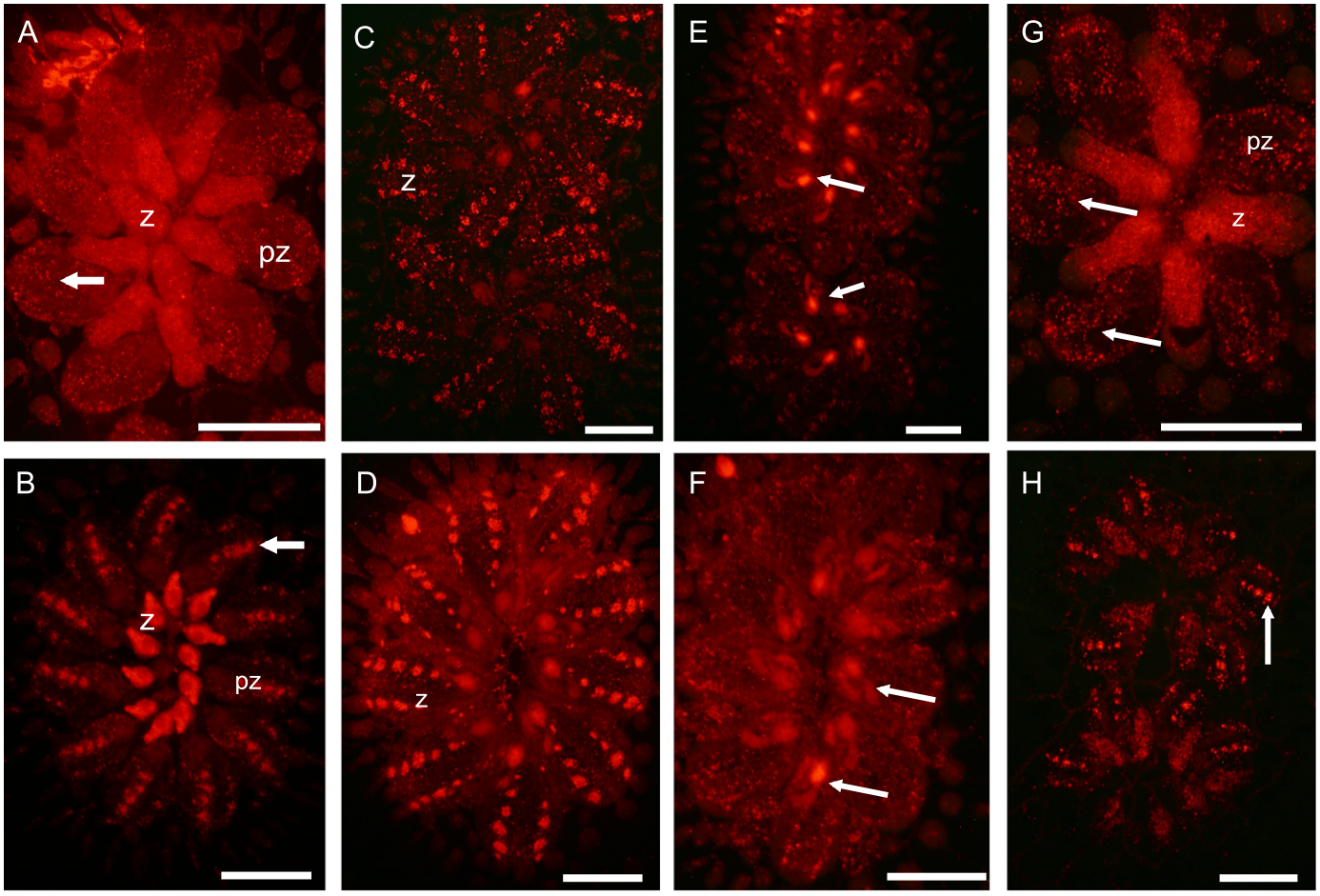

Fig. 1. Bioparticles are rapidly engulfed within VIP. Ventral view of a *B. schlosseri* colony microinjected with Alexafluor-594 *E.coli* bioparticles. ((A)–(H)) A single system colony was injected at the onset of takeover (cycle *N*) and followed throughout the blastogenetic cycle until stage 9/7/1 of cycle *N*+2. (A) Mid-takeover (cycle *N*), eight hours following microinjection: the resorbing adult zooids are intensely labeled, whereas pre-functional zooids exhibit a punctuate fluorescence pattern (arrow). (B) At twelve hours post microinjection, adult zooids have almost been completely resorbed. Fluorescent bioparticles can be clearly observed within ventral islands of pre-functional zooids (arrow). (C) Stage 9/7/1+ of blastogenetic cycle *N*+1. The fluorescent bioparticles are localized within phagocyte-rich, zooid ventral islands, which are bilaterally distributed along the antero-posterior axis of adult zooids. (D) Stage 9/8/2 (cycle *N*+1). The fluorescence pattern is prominently visible within the bilaterally distributed, zooid ventral islands along each zooid's A/P axis. (E) Stage 9/8/4 of blastogenetic cycle *N*+1. Zooid ventral islands are still visible, albeit with reduced fluorescence intensity and cellularity. During this developmental stage, fluorescence can also be observed within the zooid's digestive tract (arrows). (F) During stage 9/8/5 of blastogenetic cycle *N*+1, the fluorescent ventral islands are no longer visible as phagocytes have scattered in the colonial vasculature. The stomach and intestine from adult zooids are also fluorescently labeled (arrows), suggesting that bioparticles may gradually be excreted from the colony. (G) During takeover of blastogenetic cycle *N*+1, the dying adult zooids are intensely labeled. Conversely, a punctuate fluorescence pattern is observed within pre-functional zooids (arrow). This pattern depicts circulating, Alexafluor 594-positive phagocytes that are homing within pre-functional zooid of the next asexual generation. (H) Stage 9/7/1 of blastogenetic cycle *N*+2, showing resorbing zooids and adult zooids of the next asexual generation that have reached functional maturity. This panel depicts the formation of Alexafluor 594-fluorescent ventral islands within pre-functional zooids (arrow). As with the previous asexual generation, zooid ventral islands exhibit bilateral distribution along the A/P axis. PZ: pre-functional zooid, Z: zooid. Scale bar: 1 mm.

Please cite this article as: Lauzon, R.J., et al., Phagocyte dynamics in a highly regenerative urochordate: Insights into development and host defense. Dev. Biol. (2012), http://dx.doi.org/10.1016/j.ydbio.2012.11.006

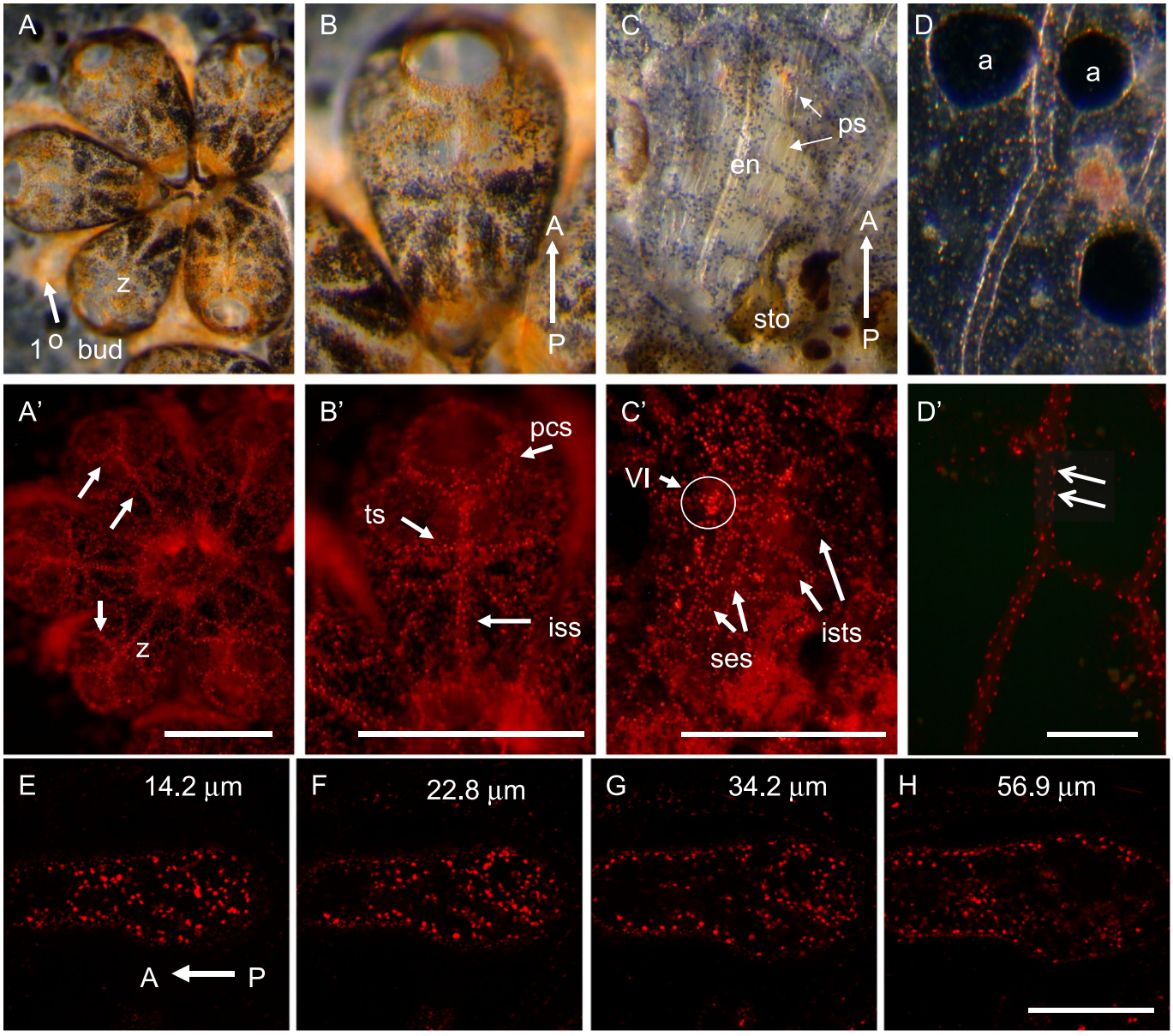

Fig. 2. Bioparticle engulfment defines a second phagocyte population that homes to zooid sinuses/lacunae (sinus/lacunae phagocytes) and extracorporeal blood vessels (vessel phagocytes). Dorsal view of a two-system, *B. schlosseri* colony that was microinjected during the takeover phase of blastogenesis with Alexafluor 594 *E. coli* bioparticles, and observed in real-time during stage 9/8/5 of the following blastogenetic cycle ($N+1$) under modified darkfield (A–D) and epifluorescence stereomicroscopy (A′–D′), respectively. (A, A′) Numerous phagocytes can be observed lining the blood sinuses of each zooid (arrows). (B, B′) Detail of an adult zooid: numerous phagocytes can be observed lining the intersiphonal sinus (iss), pericoronal sinus (pcs) and transverse sinuses (ts). (C, C′) Detail of a single adult zooid viewed in its ventral plane. Numerous phagocytes can be observed lining the interstigmatic sinuses (ists) and sub-endostylar sinuses (ses). The phagocyte-rich, ventral islands are still visible at this stage of blastogenesis, albeit with reduced cellularity. (D, D′) Detail of the marginal vessel situated at the periphery of the colony: numerous Alexafluor 594-positive phagocytes can be observed repeatedly along the vessel wall. Note the absence of fluorescent phagocytes in the ampullae and tunic matrix. ((E)–(H)) Detail of a regressing, adult zooid observed at different optical planes along its dorso-ventral axis: a single system colony was microinjected during the takeover (cycle N) and observed during mid-takeover of the following blastogenetic generation (cycle $N+1$). Panel E depicts a ventral section whereas panel H is a dorsal section: alexafluor-594$^+$ sinus/lacunae phagocytes are observed throughout the zooid's dorso-ventral axis. Unlike VIP, which continually circulate throughout takeover, sinus phagocytes are static cells that remain within the regressing zooids throughout takeover Am: ampulla; P→A: antero-posterior axis; en: endostyle; ps: pharyngeal slits; sto: stomach; VI: ventral island; z: zooid. Scale bars: 1 mm (A–C and A′–C′), 100 um (D–D′) and 250 µm ((E)–(H)), respectively.

decreased thereafter (Suppl. Fig. 2A′–D′). Moreover, VIP displayed a conspicuous orange pigment irrespective of whether the colonies had been microinjected with fluorescent bioparticles or not, and their disappearance from the VI could also be monitored under darkfield stereomicroscopy (Suppl. Fig. 2A–D). These findings suggest that the VIP are mobile cells and that the ventral islands are themselves dynamic structures that are constantly remodeled during cyclic blastogenesis.

Throughout these experiments, phagocytes were also observed in the zooid sinuses and lacunae throughout the zooid body at all phases of blastogenesis (Fig. 2). In the dorsal plane of adult zooids, numerous phagocytes were observed lining the major sinuses, including the intersiphonal, pericoronal and transverse sinuses (Fig. 2A, B and 2A′, B′). Phagocytes were also observed lining the interstigmatic and sub-endostylar sinuses in the ventral plane of adult zooids as well as lacunae surrounding the zooid's viscera (Fig. 2C and C′). Alexafluor-594$^+$ phagocytic cells were consistently observed lining the marginal vessel at the colony's periphery and other extra-corporeal blood vessels, but were absent in the tunic matrix (Fig. 2D and D′). Using confocal microscopy, we

Please cite this article as: Lauzon, R.J., et al., Phagocyte dynamics in a highly regenerative urochordate: Insights into development and host defense. Dev. Biol. (2012), http://dx.doi.org/10.1016/j.ydbio.2012.11.006

further demonstrated that Alexafluor-594^{+}, sinus/lacunae phagocytes were localized throughout the zooid's dorso-ventral axis during takeover (Fig. 2E–H). Together, these findings suggest that *B. schlosseri* colonies harbor two distinct phagocyte populations that occupy distinct micorenvironments.

Morphology and selectivity of phagocyte populations

Histological and ultrastructural analysis was subsequently carried out to investigate the characteristics of phagocyte populations. In hematoxylin & eosin-stained tissue sections, VI were observed bilaterally within the blood space delineated by the peribranchial epithelium and epidermis, and were in the same sectional plane as the sub-endostylar sinus, in the ventral plane of adult zooids (Suppl. Fig. 3A and B). The fixed phagocyte populations lining zooid lacunae/sinuses and colonial blood vessels (from this point on, these cells will be collectively referred to as vessel phagocytes) could not be distinguished histologically from other cells. Using transmission electron microscopy, we consistently observed that VIP contained numerous phago-lysosomes (Fig. 3A) and appeared morphologically identical to the macrophage-like cells previously described (Lauzon et al., 1993; Burighel and Schiavinato, 1984; Ballarin et al., 2008). Most of these cells exhibited tight clustering and extensive membrane contact with each other (Fig. 3B). The vessel phagocytes were found to display an extensive area of cytoplasmic membrane contact with the basal lamina (Fig. 3C), contained prominent intra-cytoplasmic vesicles and Golgi apparatus. However, phagolysosomes were not always visible (Fig. 3D).

In order to determine functional properties (i.e., the selectivity) of ventral island and vessel phagocyte populations, colonies were microinjected with diverse substrates, including India ink carbon particles, Alexafluor-conjugated *Staphyloccus aureus* and *S. cerevisiae* (yeast) bioparticles, Alexafluor-conjugated carboxylated microspheres (1 μm in diameter) and BODIPY-fluorescent PBS liposomes (ranging in diameter between 5 and 15 μm) (Suppl. Table 1; Suppl. Figs. 3 and 4). Ventral island phagocytes consistently engulfed India ink (carbon) particles (Suppl. Fig. 3C and D), Alexafluor-conjugated, Gram positive bacteria (*S. aureus*) (Suppl. Fig. 3E and F), *S. cerevisiae* yeast bioparticles (Suppl. Fig. 3G), carboxylated microspheres and liposomes (Suppl. Table 1 and Suppl. Fig. 4A and A′). In contrast, vessel phagocytes were only found to engulf carbon particles, Gram positive and negative bacteria (Suppl. Table 1; Suppl. Fig. 3G; Suppl. Fig. 4A–A′,

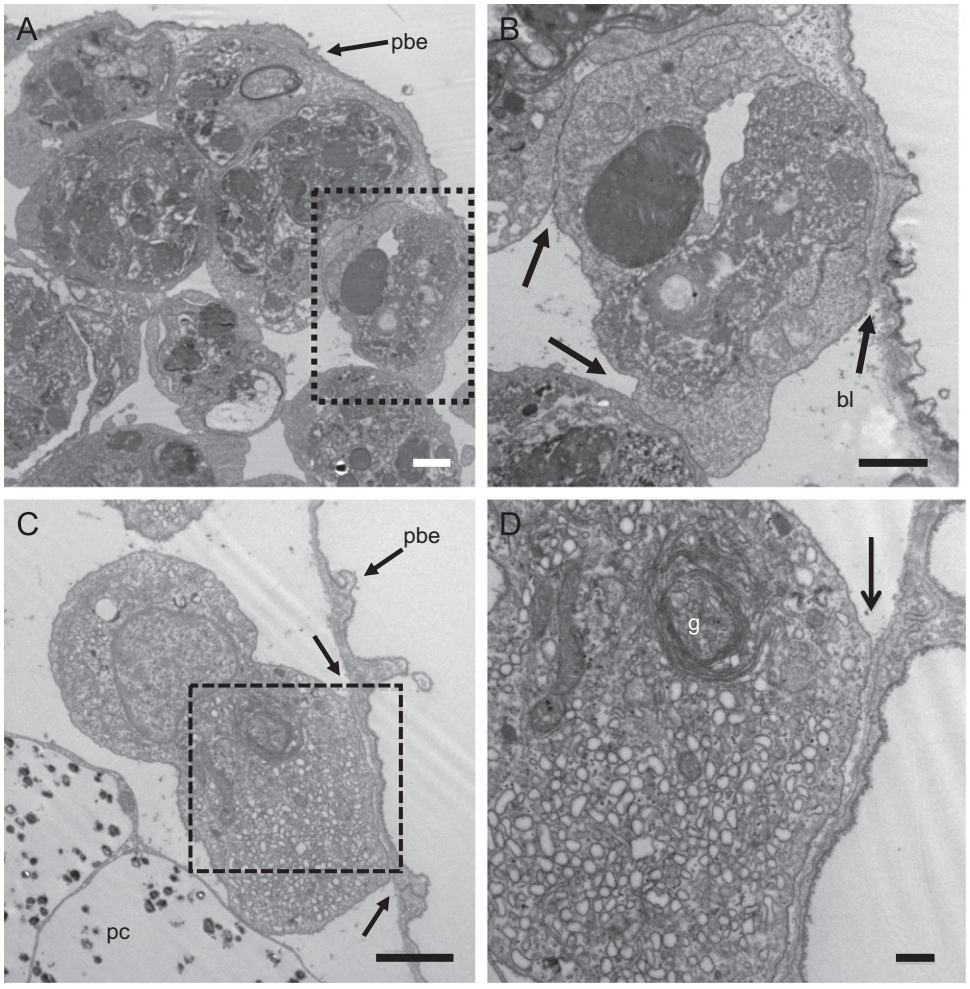

Fig. 3. Ultrastructural analysis of zooid ventral islands. Ultrathin section of VIP during stage 9/7/1+. (A) Ventral island (VI) phagocytes contain phago-lysosomes and appear morphologically identical to macrophage-like cells previously described in the literature (Burighel and Schiavinato, 1984; Lauzon et al., 1993; Ballarin et al., 2008). These cells exhibit tight homotypic clustering and extensive cell-cell contact. A few of the phagocytes interact with the basal lamina of the peribranchial epithelium. (B) High magnification of the boxed area from panel A depicting a VI phagocyte interacting with neighboring VI phagocytes (arrows), and with the basal lamina of the peribranchial epithelium. (C) Blood cell thought to be a sinus phagocyte exhibiting extensive area of cytoplasmic membrane contact with basal lamina of a zooid sinus near a ventral island (arrows). This cell displays a prominent Golgi apparatus and cytoplasmic vacuoles. (D) High magnification of boxed area from panel C depicting the region of cytoplasmic membrane contact with the basal lamina. Bl: basal lamina; g: Golgi apparatus; pbe: peribranchial epithelium. Scale bars: 25 μm (A), 2 μm ((B) and (C)) and 500 nm (D).

Please cite this article as: Lauzon, R.J., et al., Phagocyte dynamics in a highly regenerative urochordate: Insights into development and host defense. Dev. Biol. (2012), http://dx.doi.org/10.1016/j.ydbio.2012.11.006

B′B′). When microinjected simultaneously with *E. coli* bioparticles, engulfed BODIPY PBS liposomes co-localized with the bioparticles in the VI phagocytes (Suppl. Fig. 4C–E). Interestingly, a similar phagocyte localization pattern within VI, sinuses/lacunae and blood vessels was observed in *Botrylloides violaceus* colonies microinjected with Alexafluor 594-conjugated *E. coli* bioparticles (Suppl. Fig. 3H and I). Thus, we can distinguish populations based on selective phagocytosis.

Only VIP can move between histocompatible colonies and retain their behavior

Up to this point, our findings suggest that VIP are mobile cells that circulate in the colonial vasculature, and display homing properties that enable them to move from one blastogenetic cycle to the next (Fig. 1). In contrast, vessel phagocytes exhibit distinct homing properties. In order to investigate the properties exhibited by these two distinct cell populations, experimental parabiosis experiments were carried out using histocompatible, clonal replicate colonies. It is well documented that genetically identical *B. schlosseri* colonies readily undergo vascular fusion following ampullar contact (Scofield et al., 1982; Saito et al., 1994; Weissman, 2000; De Tomaso et al., 2005). In order to track VIP and vessel phagocyte populations, single system clonal replicate colonies were microinjected individually with either Alexafluor 488 or 594 *E. coli* bioparticles and experimentally fused during blastogenetic cycle *N* (Fig. 4A). Observations were carried out during blastogenetic cycles $N+1$ and $N+2$ in both the Alexafluor 488 (green fluorescent) and Alexafluor 594 (red fluorescent) fusion partner. Representative data is shown only for the Alexafluor 488 fusion partner (Fig. 4B–B″, C–C″). At the onset of takeover during cycle $N+1$, Alexafluor 594^{+} mobile phagocytes consistently aggregated and co-localized with Alexafluor 488^{+} VIP within the VI (Fig. 4B, B′, B″). In contrast, only Alexafluor 488^{+} vessel phagocytes were observed in the fusion partner microinjected with Alexafluor 488 bioparticles. Conversely, only Alexafluor 594^{+} vessel phagocytes were observed in the blood vessels and sinuses of the fusion partner microinjected with Alexafluor

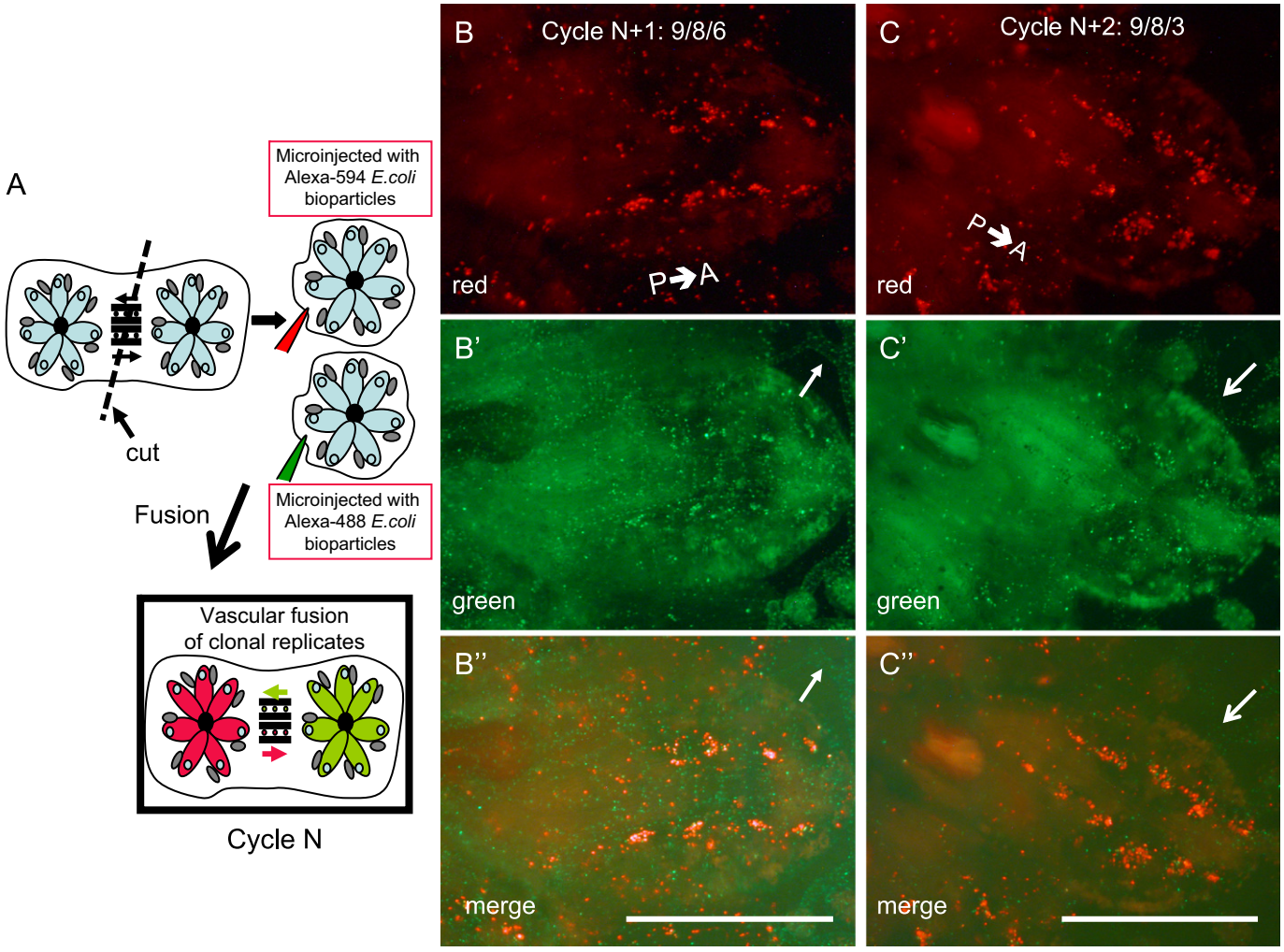

Fig. 4. VIP are mobile whereas sinus/lacunae and vessel phagocytes are static in vascular parabionts. (A) Diagram and picture of two *B. schlosseri* clonal replicates that have been experimentally separated and microinjected with Alexafluor 594 and Alexafluor 488 *E. coli* bioparticles,during stage 9/7/1 of cycle *N*. Single-system, clonal replicates were subsequently joined by experimental parabiosis. The bidirectional arrows depict the flow of green and red fluorescent, mobile phagocytes in colonies following vascular fusion. (B–C″): Alexafluor 488 *E. coli* microinjected clonal replicate observed under real-time, epifluorescence stereomicroscopy following vascular fusion, at onset of takeover of cycle $N+1$ (B–B″) and stage 9/8/2 of cycle $N+2$ (C–C″), respectively. Panels B–B″ and C–C″ depict ventral views from a single adult zooid observed using a 620 nm emission filter (red; B, C), 522 nm emission filter (green; B′, C′) and merged images (B″, C″). The mobile phagocytes from the Alexafluor 594 labeled (red) fusion partner have homed to the zooid ventral islands and aggregated with the remaining VI phagocytes of the Alexafluor 488-labeled (green) fusion partner. In contrast, sinus/lacunae phagocytes and vessel phagocytes (arrows) are exclusively from the Alexafluor 488-labeled (green) fusion partner. During blastogenetic cycle $N+2$, red and green fluorescent VI phagocytes are co-localized within the zooid VI (C–C″). Moreover, few sinus/lacunae phagocytes can be observed within the sinuses and lacunae of the Alexafluor 488-labeled (green fluorescent) adult zooid (C′). In contrast, vessel phagocytes can still be observed exclusively from the Alexafluor 488-labeled fusion partner (C′–C″). P→A: antero-posterior axis. Scale bars: 1 mm.

Please cite this article as: Lauzon, R.J., et al., Phagocyte dynamics in a highly regenerative urochordate: Insights into development and host defense. Dev. Biol. (2012), http://dx.doi.org/10.1016/j.ydbio.2012.11.006

594 bioparticles (data not shown). During blastogenetic cycle $N+2$, red and green fluorescent VIP co-localization was observed within the VI of the Alexafluor 488 fusion partner (Fig. 4C, C′, C″). Interestingly, Alexafluor 488$^+$ vessel phagocytes could only be consistently observed within the extracorporeal blood vessels. Few if any, were observed within the sinuses and lacunae of the Alexafluor 488 fusion partner (Fig. 4 C, C′, C″).

We further investigated the homing behavior of VIP in colonies microinjected with BODIPY red PBS liposomes, using vascular parabiosis of histocompatible colonies. As described in the previous section, liposomes were selectively engulfed by VIP (Suppl. Fig. 4). In these experiments, one clonal replicate was microinjected with BODIPY red PBS liposomes at the onset of blastogenetic cycle *N*, and subsequently fused with an unlabeled fusion partner (Suppl. Fig. 5A). BODIPY red$^+$, mobile phagocyte were subsequently tracked in this recipient colony during blastogenetic cycle *N* and $N+1$. Following vascular fusion, in the early stages of takeover of cycle *N*, mobile phagocytes began to appear in the recipient colony (Suppl. Fig. 5B and B′). By mid-takeover, BODIPY red$^+$ VIP aggregated within the recipient's VI of the pre-functional zooids (Suppl. Fig. 5C and D), and adult zooids during blastogenetic cycle $N+1$ (Suppl. Fig. 5E and E′). As expected, no BODIPY red$^+$, sinus/lacunae phagocytes could be observed along the dorso-ventral plane of the recipient adult zooids during either cycle *N* or $N+1$ (Suppl. Fig. 5D, E–E′, F–F′). Collectively, these findings strongly suggest that VIP are mobile cells that utilize the colonial vasculature to home from one generation to the next, whereas vessel phagocytes appear to be a static population.

Fate of the mobile and the static phagocyte populations: Recycling vs. turnover

In order to better understand the fate of both phagocyte populations from one asexual generation to the next, we investigated their behavior using high resolution, confocal microscopy imaging. Specifically, we addressed the following questions: are mobile phagocytic cells recycled and reutilized from one blastogenetic generation to the next, or are they subject to turnover within the VI? Second, what is the fate of sinus/lacunae phagocytes within regressing adult zooids? To address the first question specifically, mobile, VIP were tracked in vascular parabionts that had been previously microinjected in blastogenetic cycle *N* with either Alexafluor 488 or 594 *E. coli* bioparticles. Two possible models could account for the observed behavior of mobile phagocytes in our study: the recycling model predicts that mobile VIP from both fusion partners co-localize within the VI during blastogenetic cycle $N+1$ and retain their individual characteristics; that is Alexafluor 488$^+$ and Alexafluor 594$^+$ remain distinct from one another within the VI (Suppl. Fig. 6A). In contrast, the turnover model predicts that Alexafluor 488$^+$ and Alexafluor 594$^+$ VIP are engulfed by a newly-born population of phagocytic cells as early as cycle $N+1$, and these 'new' cells become the next functional generation of ventral island phagocytes (Suppl. Fig. 6B).

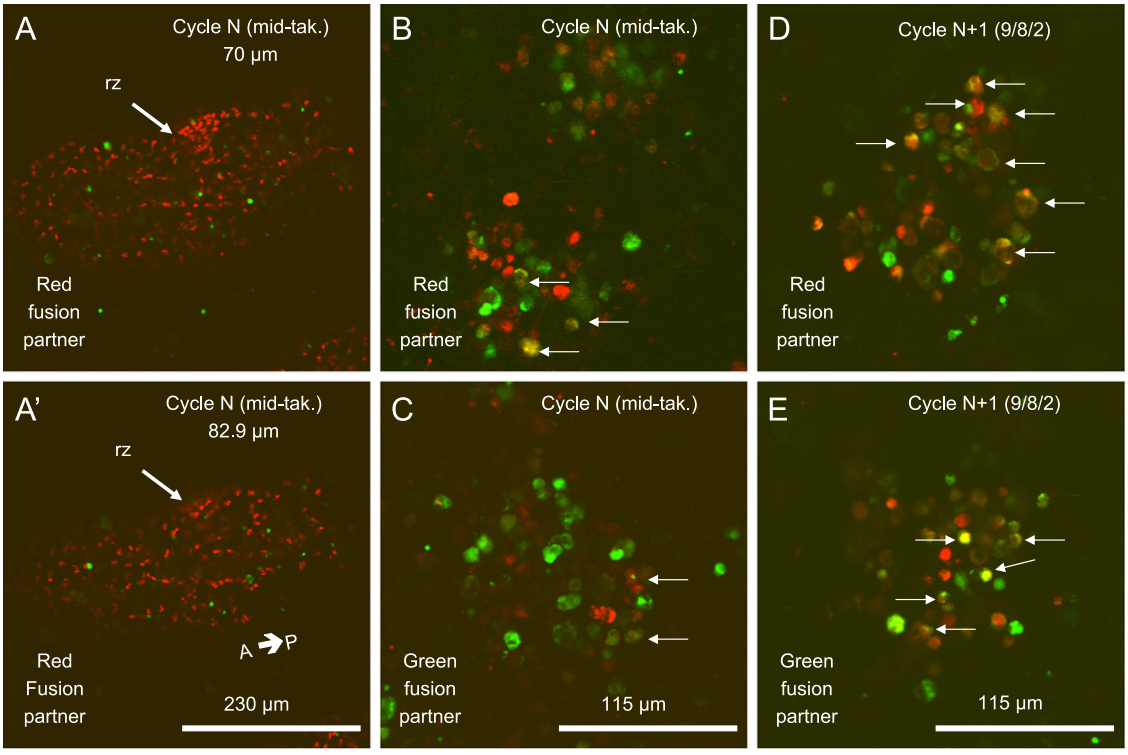

Fig. 5. Phagocyte dynamics and turnover following experimental parabiosis. Single system *B. schlosseri* clonal replicates were microinjected, respectively with Alexafluor 594 and Alexafluor 488 *E. coli* bioparticles, subsequently joined by experimental parabiosis, and observed under real-time confocal microscopy. (A–A′) Mid-takeover, regressing adult zooid from the fusion partner microinjected with Alexafluor 594 bioparticles, observed at two different optical planes along its dorso-ventral axis during blastogenetic cycle *N*. The position along the zooid's optical plane is indicated at the top right corner of each panel. Panel A′ depicts a ventral section. The mobile phagocytes from the Alexafluor 488 fusion partner (green) can be seen amidst the static, Alexa 594$^+$ sinus phagocytes within regressing zooids. No co-localization of the fluorescent labels in sinus/lacunae and mobile phagocytes can be observed. (B–C) Detail of a VI from the pre-functional zooid observed in the fusion partners microinjected with Alexafluor 594 *E. coli* bioparticles (B) and Alexafluor 488 *E. coli* bioparticles (C), respectively. The majority of VI phagocytes exhibit either green or red fluorescence. A few VI phagocytes can be observed which display dual green and red fluorescence (arrows), indicative of turnover. (D–E) Detail of a VI from the pre-functional zooid at stage 9/8/2 of cycle $N+1$, observed in the fusion partners microinjected with Alexafluor 594 *E. coli* bioparticles (D) and Alexafluor 488 *E. coli* bioparticles (E), respectively. The majority of VI phagocytes can now be observed which display dual green and red fluorescence (arrows), indicative of a high level of turnover. P→A: antero-posterior axis; rz: regressing zooid. Scale bars: 230 µm (A–A′) and 115 µm (B–C and D–E), respectively.

Please cite this article as: Lauzon, R.J., et al., Phagocyte dynamics in a highly regenerative urochordate: Insights into development and host defense. Dev. Biol. (2012), http://dx.doi.org/10.1016/j.ydbio.2012.11.006

In order to distinguish between both models of phagocyte cell behavior (recycling vs. turnover), confocal microscopy imaging was carried out during blastogenetic cycles *N* and *N*+1 in both the Alexafluor 488 (green fluorescent) and Alexafluor 594 (red fluorescent) fusion partner. During mid-takeover of cycle *N*, we consistently observed few mobile Alexafluor 488+ phagocytes among numerous, static Alexafluor 594+ cells throughout the dorso-ventral axis of adult zooids within the Alexafluor 594 fusion partner (Fig. 5A and A′), and vice versa for the Alexafluor 488 fusion partner (data not shown). Interestingly, there was no co-localization of fluorescent label for sinus/lacunae and mobile phagocytes in these vascular parabionts. Moreover, the sinus/lacunae phagocytes remained fixed within the regressing zooids throughout the duration of takeover, as determined under real-time, confocal imaging of the same zooids repeatedly observed throughout takeover (data not shown). In the ventral islands of the pre-functional zooids, the great majority of VI phagocytes exhibited either green or red fluorescence. A few VI phagocytes were consistently observed to display dual green and red fluorescence in either fusion partner (Fig. 5B and C). In contrast, by stage 9/8/2 of blastogenetic cycle *N*+1, most VIP displayed dual green and red fluorescence in either the Alexafluor-488 or −594 fusion partners, indicative of phagocytic cell turnover within VI (Fig. 5D and E). Next, we carried out an ultrastructural analysis of VI using transmission electron microscopy in order to confirm these observations. In the early stages of the blastogenetic cycle (9/7/1+), phagocytes exhibiting lesions in their cytoplasmic membrane were observed amidst other VIP (Fig. 6A and B). Moreover, damaged phagocytes were consistently observed being engulfed by other phagocytes within the VI, often using a dynamic, tag-team approach in which the pseudopodia of both active phagocytes overlapped extensively with each other (Fig. 6C and D).

Next, we hypothesized that the observed tag-team strategy of phagocytic cell engulfment of effete phagocytes could possibly reveal the VI to also function as sites for recruitment of newly born and mitotically active phagocytes. Thus, in order to investigate whether some VIP were mitotically active, single system colonies were microinjected with pHrodo *E. coli* biopaticles and subsequently processed 24 h later under whole mount immunohistochemistry with a monoclonal antibody against phospho histone H3 (pHH3) to detect mitotic cells. pHrodo fluorescence withstands paraformaldehyde fixation and was used in these experiments to determine whether pHrodo staining and Alexafluor-488 pHH3 immunoreactivity co-localized. Alexafluor 488^{+} mitotic cells were observed, scattered in the zooid ventral

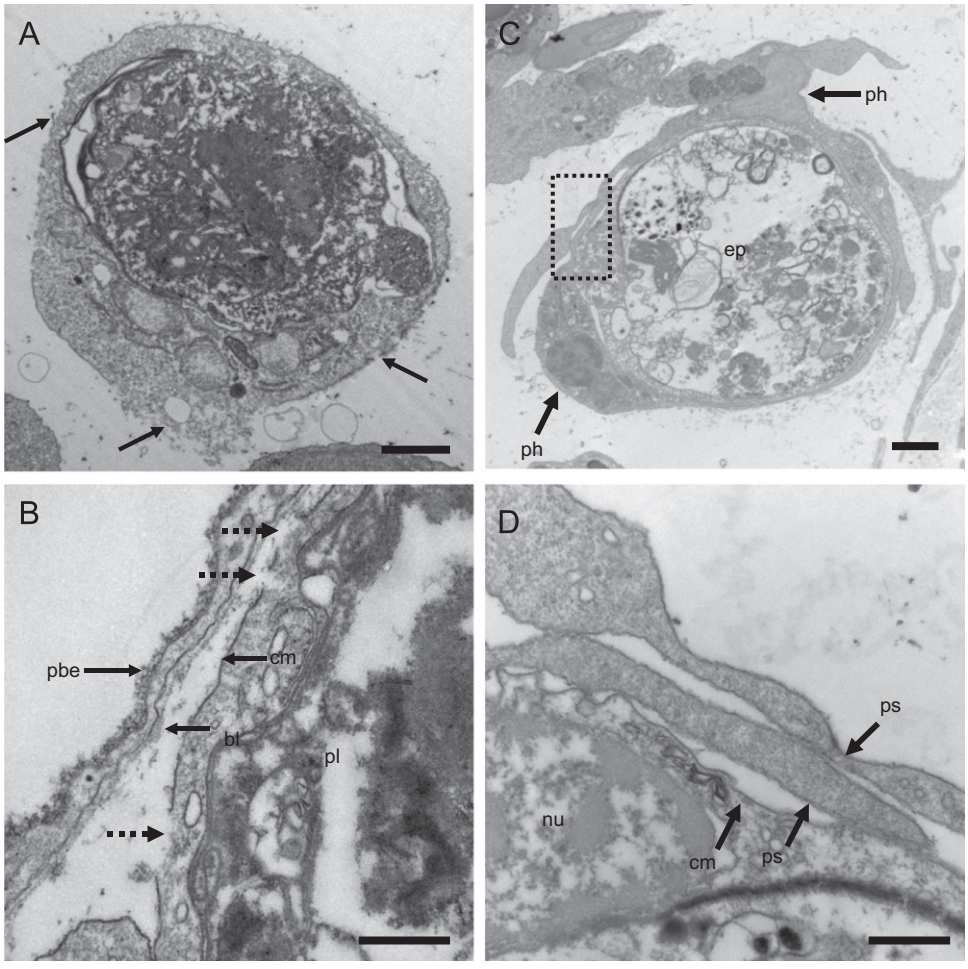

Fig. 6. Turnover of VIP during cyclic blastogenesis in *B. schlosseri*. Transmission electron micrographs of VI phagocytes at stage 9/7/1+. (A) Damaged phagocyte at the edge of a ventral island. The cytoplasmic membrane is ruptured at many sites along the cell surface (black arrows). (B) Detail of a damaged VI phagocyte interacting with the basal lamina of the peribranchial epithelium. Note the discontinuity of the phagocyte's cytoplasmic membrane along multiple sites (dashed arrows). (C) VI macrophage being actively engulfed by two smaller phagocytic cells. (D) Detail of the dashed rectangular area highlighted in panel C. Pseudopodia of both active phagocytes interact with each other (arrows) and promote a dynamic tag-team approach to the engulfment process. The nucleus of the engulfed macrophage is also shown, and reveals condensation and margination of the chromatin against the nuclear membrane, indicative of apoptosis. Bl: basal lamina of peribranchial epithelium; cm: cytoplasmic membrane; ep: engulfed phagocyte; nu: nucleus; ph: phagocyte; pbe: peribranchial epithelium; pl: phago-lysosome; ps: pseudopodium. Scale bars 2 μm ((A) and (C)) and 500 nm ((B) and (D)).

Please cite this article as: Lauzon, R.J., et al., Phagocyte dynamics in a highly regenerative urochordate: Insights into development and host defense. Dev. Biol. (2012), http://dx.doi.org/10.1016/j.ydbio.2012.11.006

sinuses and within the developing primary bud (Fig. 7A and B) as well as the male germline in both adult zooids and primary buds (data not shown). In contrast, pHrodo$^+$ VIP were phospho-histone H3$^-$. There was no co-localization of pHrodo fluorescence and pHH3 immunoreactivity, as observed under confocal microscopy (Fig. 7B and C). In western blots, the pHH3 monoclonal antibody detected a single polypeptide band at 17 kD in both blastogenetic stage B1 *B. schlosseri* lysates and the control HT-2 mammalian cell lysate (Fig. 7). Collectively, these findings are consistent with the turnover model and strongly suggest that VI are sites of turnover of non-mitotic, mobile phagocytes.

Motility of VIP Is not affected by complete budectomy

We have previously demonstrated that surgical removal of developing buds in a colony (complete budectomy) fails to prevent zooid death, but effectively curtails zooid resorption during takeover, and that a single, primary bud is sufficient to rescue the ability of an adult zooid to be effectively resorbed, albeit with delayed kinetics (Lauzon et al., 2002). Moreover, it is well documented that circulating phagocytes are important effectors in zooid resorption (Burighel and Schiavinato, 1984; Lauzon et al., 1993, 2002; Voskoboynik et al., 2004). Therefore, we investigated whether budectomy affected phagocyte dynamics and homing in *B. schlosseri* colonies. One hour following complete budectomy (consistently carried out during stage 9/8/2 of blastogenesis to minimize bud regeneration which frequently occurs if buds are surgically removed during stages 9/7/1 or 9/7/1$^+$), ventral islands phagocytes (VIP) containing engulfed *E. coli* bioparticles were localized within the VI (Fig. 8A and A′). At twenty four hours post-budectomy, VI were still prominent morphologically, albeit with decreased numbers of Alexafluor$^+$ VIP (Fig. 8B and B′). At thirty-six hours, VIP density within the VI had greatly decreased (Fig. 8C and C′) and paralleled the mobility patterns observed in control clonal replicate colonies (data not shown). Twelve hours following siphon shutdown and zooid contraction during takeover, VI were no longer visible and mobile phagocytes were scattered within regressing zooids and throughout the colonial vasculature (data not shown). In contrast, sinus/lacunae phagocytes were prominently observed along the antero-posterior axis of regressing adult zooids (Fig. 8D and D′). Since these observations are similar to that seen in non-surgically manipulated, control colonies, the findings are consistent with the notion that phagocyte dynamics during a given blastogenetic cycle is a bud independent process.

A single bud Is sufficient to rescue the VIP homing cycle

In order to investigate the functional involvement of buds in phagocyte homing from one asexual generation to the next, hemi-budectomies were carried out in which a single primary bud was allowed to grow and mature. We have previously shown that under such conditions, the primary bud grows to a size that exceeds the original buds in the colony present, undergoes cellular hyperplasia and becomes a so-called superzooid (Lauzon et al., 2002; Kürn et al., 2011). In colonies microinjected with Alexafluor 594 *E. coli*

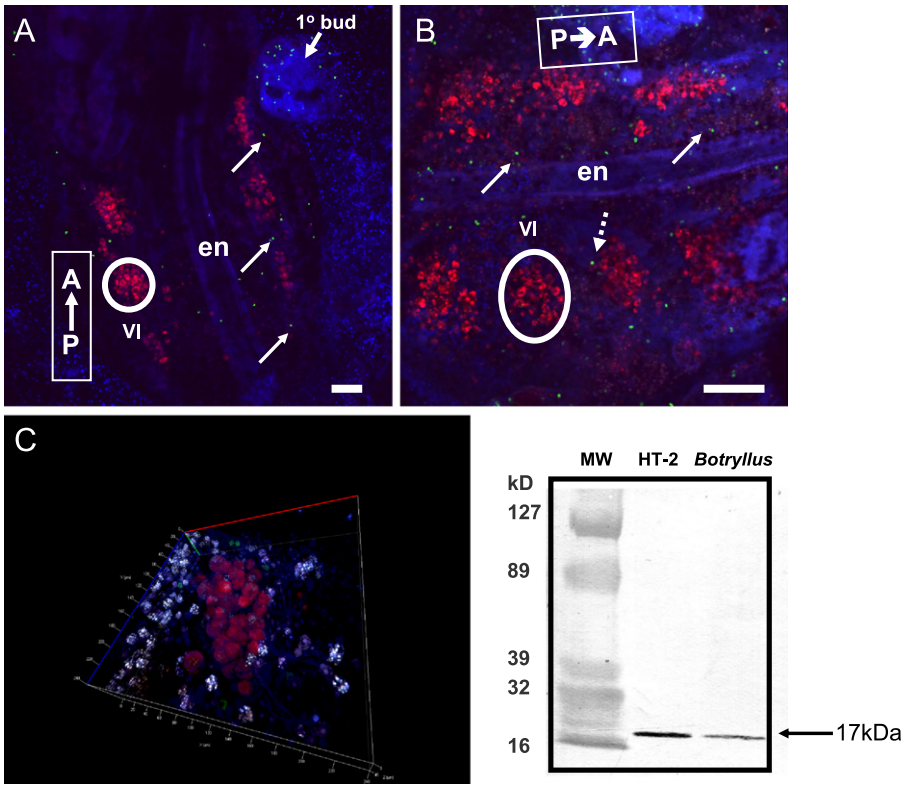

Fig. 7. VIP are non-mitotic cells. A single system colony was microinjected with pHrhodo *E. coli* bioparticles and 24 h after, stained with a rabbit polyclonal antibody directed against phospho histone H3 (green). (A) Whole mount of adult zooid counterstained with DAPI, at stage 9/8/2. Mitotic cells (green) are observed scattered in the zooid ventral sinuses (white arrows) and within the developing primary bud. pHrhodo-labeled, VI can also be seen and display red fluorescence (white circle). (B) Detail of adult zooid. Phospho-histone H3$^+$ cells are observed lining the sub-endostylar sinus (white arrows) and scattered within the developing primary bud. In contrast, pHrhodo-labeled, VI phagocytes are phospho-histone H3$^-$. Mitotic cells are occasionally seen at the edge of a ventral island (dashed arrow). (C) Confocal three-dimensional reconstruction of a VI. VI phagocytes (red) are phospho histone H3$^-$. (D) Western blot analysis of lysates from cultured mouse HT-2 cells (20 μg) grown in the presence of interleukin-2 and a stage 9/8/2 *B. schlosseri* colony (40 μg), probed with a primary, rabbit polyclonal antibody against phospho histone H3. Note the presence of a single polypeptide band at 17 kDa in both mammalian and *Botryllus* lanes. A→P: Antero-posterior axis of adult zooid; en: endostyle; MW: molecular weight markers; VI: ventral island. Scale bar: 100 μm.

Please cite this article as: Lauzon, R.J., et al., Phagocyte dynamics in a highly regenerative urochordate: Insights into development and host defense. Dev. Biol. (2012), http://dx.doi.org/10.1016/j.ydbio.2012.11.006

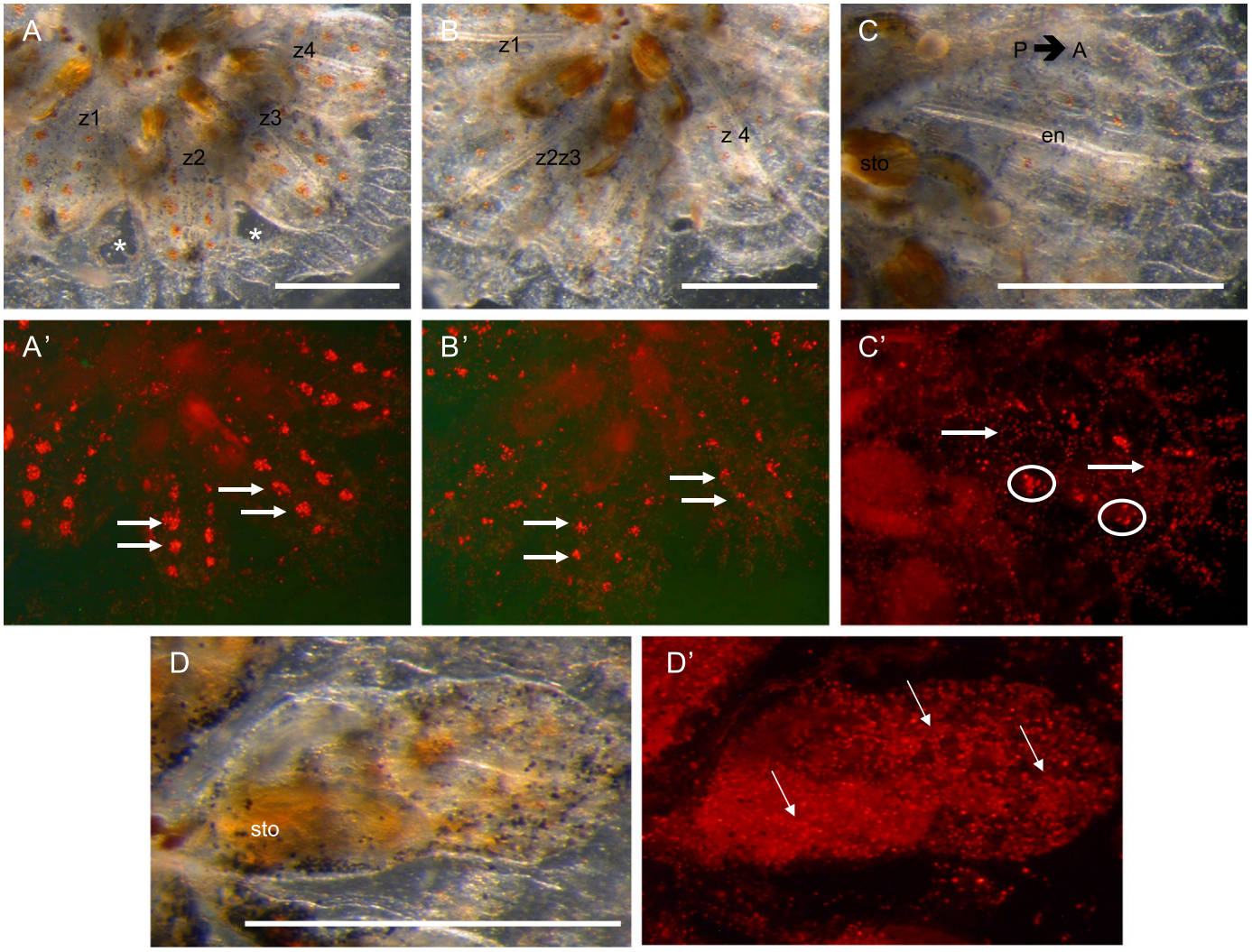

Fig. 8. VIP recirculate normally following complete budectomy. Complete budectomy on a single system colony of seven zooids during stage 9/8/2 and observed in real-time under modified darkfield microscopy (panels A–D) and epifluorescence stereomicroscopy (panels A′-D′), respectively. (A, A′) A portion of the colony one hour following budectomy: four adult zooids can be seen (z1–z4), each of which exhibit bilaterally distributed ventral islands (arrows). The locations where buds were surgically removed, are indicated by asterisks. (B, B′) The same colony, 24 h following budectomy: VI are still visible, albeit with reduced phagocyte cellularity (arrows). (C, C′) Detail of a single zooid, 36 h following budectomy. VIP (encircled areas) are still visible as are the sinus phagocytes (arrows). (D, D′) Detail of a single zooid at 12 h post-onset of takeover. Ventral islands are no longer visible, whereas fixed (sinus/lacunae) phagocytes are observed throughout sinuses and lacunae of the regressing zooid (arrows). P→A: antero-posterior axis; en: endostyle; sto: stomach. Scale bars: 1 mm.

bioparticles ($N=10$), VI containing Alexafluor^{+} VIP gradually appeared, and were observed throughout superbud development and within the superzooid (Fig. 9 A-D and A′-D′). Interestingly, both superbuds and superzooids expressed additional ventral islands bilaterally (range of 6–8 vs. 4–5 in control colonies per adult zooid) as well as supernumerary islands lateral to the main ventral islands (Fig. 9C′ and D′). Using confocal microscopy imaging, we further observed an increase in ventral island phagocyte cellularity within superbuds and superzooids (data not shown).

Knockdown of VIP delays the resorption phase of adult zooids during takeover

We sought to determine the functional involvement of VIP in colony wide homeostatic events, including bud development, zooid death and regression during takeover. In order to specifically target VIP, BODIPY red liposomes containing the phagocidal drug clodronate (dichloromethylene biphosphonate) were microinjected in small, single or double system colonies at various stages of blastogenesis ($N=36$). Clonal replicate, control colonies were simultaneously microinjected with BODIPY red PBS liposomes ($N=29$) and specific colony-wide parameters were compared between both experimental groups of colonies (Fig. 10, Table 1). In clodronate liposome colonies, blastogenesis proceeded with normal temporal kinetics in the days following microinjection. All of the colonies initiated takeover normally (zooid contraction, siphon closure and loss of responsiveness to mechanical stimuli), but zooid regression and involution were delayed in the great majority of cases (30 of 36 colonies; 83.3%) when compared with PBS liposome colonies (Table 1; Fig. 10A–F). In contrast, only 6.9% of PBS liposome microinjected colonies (2 of 29) displayed a (slight) delay in zooid resorption (Table 1). Interestingly, the growth of pre-functional zooids was impaired in 61.1% of clodronate liposome colonies (22 of 36), and these colonies (63.9%; 23 of 36) also produced visible delays in primary and secondary bud development (Table 1; Fig. 10I). Ampullar constriction and retraction were further noted in 44.4% (16 of 36) of the colonies. Interestingly, while evidence of VI phagocyte homing and localization was observed within ventral islands of pre-functional zooids, many VIP were atypically observed within the ventral islands of

Please cite this article as: Lauzon, R.J., et al., Phagocyte dynamics in a highly regenerative urochordate: Insights into development and host defense. Dev. Biol. (2012), http://dx.doi.org/10.1016/j.ydbio.2012.11.006

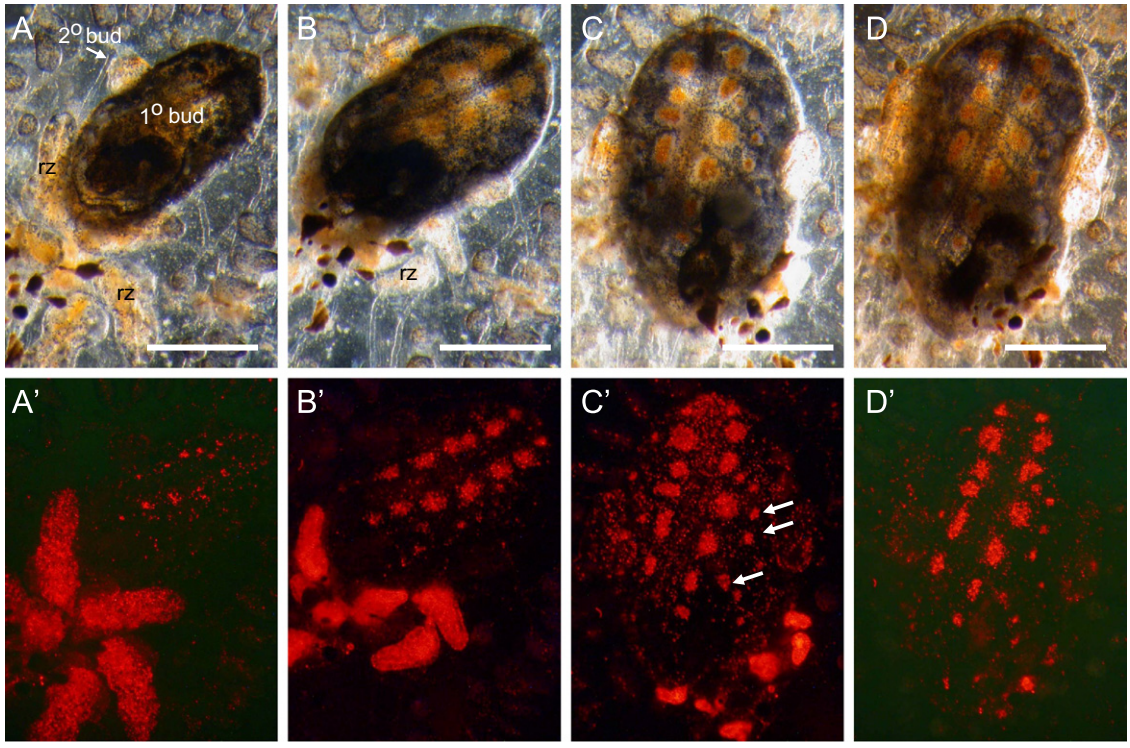

Fig. 9. A single bud is sufficient to rescue phagocyte homing to zooid ventral islands following takeover. Hemi-budectomy on a single system colony of six zooids during stage 9/8/2, leaving only a single primary bud (and associated secondary bud). The colony was subsequently observed in real-time under modified darkfield microscopy (panels A–D) and accompanying epifluorescence microscopy (panels A′–D′), respectively. (A, A′) Hemi-budectomized colony, during mid-takeover of the same blastogenetic cycle (cycle *N*) following injection. Adult zooids of the previous asexual generation are undergoing resorption and ventral islands have begun to form in the primary bud (pre-functional zooid). (B, B′) Stage 9/7/1+ of cycle *N*+1: old zooids have undergone further resorption and bilaterally-distributed ventral islands are clearly visible in the adult zooid. Note that as the lone surviving bud grows and resorbs the six adult zooids, it becomes a functionally mature, adult zooid that reaches a size that exceeds the size of normal adult zooids. In addition, this superzooid expresses additional ventral islands on either side of the endostyle. (C, C′) Stage 9/8/4 of blastogenetic cycle *N*+1: old zooids are almost completely resorbed. Phagocyte cellularity is increased in the ventral islands and within the blood sinuses of the superzooid. Supernumerary islands can also be observed (arrows). ((D) and (D′)) Stage 9/8/5 of cycle *N*+1: unlike the pattern observed in non-surgically treated, control colonies, ventral islands are still visible in the superzooid at this stage of blastogenesis. Rz: resorbing zooid. Scale bars: 1 mm.

regressing adult zooids (Fig. 10G). In the next blastogenetic cycle, VIP were still observed as discrete aggregates within the ventral islands of unresorbed zooids of the previous generation (Fig. 10H). Clodronate liposomes were well tolerated, in that only one of the thirty six microinjected colonies died from this treatment (2.8%), and the knockdown phenotype was transient, most often lasting a single blastogenetic generation, after which affected colonies resumed normal development (Table 1). Collectively, these findings suggest that VIP are instrumental to the execution of colony-wide growth and homeostatic events.

Discussion

Phagocytosis is a fundamental process in the life histories of multicellular animals, which plays a critical role in immunological, homeostatic and developmental processes (Tauber, 2003; Hume, 2006; Henson and Hume, 2006; Chang, 2009). In this study, we used the colonial ascidian *B. schlosseri* to identify and describe the behavior of phagocytic cells in a naturally occurring model of whole-body regeneration which involves cyclical, highly coordinated waves of organismal apoptosis and programmed cell clearance of cell corpses by circulating phagocytes (Lauzon et al., 2002, 2007; Kürn et al., 2011). Using microinjection of fluorescent bioparticles in the colonial vasculature, we show for the first time that circulating phagocytes can be tracked in real-time over several blastogenetic cycles. Our findings indicate that *B. schlosseri* colonies express two distinct populations of phagocytes with different behavior and substrate specificity: one is fixed, anchored to the epithelia of the peripheral vasculature, sinuses and lacunae of adult zooids, and the second moves freely through the vascular system and is endowed with homing properties to ventral mesenchymal islands (VI). The VI consist of discrete cellular aggregates that are continuous with the inner vasculature of adult zooids, and which exhibit bilateral distribution along the A/P axis of adult zooids flanking the endostyle. Both populations are non-mitotic, suggesting that they have adopted a terminally differentiated state. VIP were found to express broad phagocytic function, and were capable of ingesting Gram positive and Gram negative bacteria, yeast cells, carbon particles, carboxylated microspheres and liposomes. Conversely, sinus/lacunae and vessel phagocytes expressed a more restricted phagocytic potential, and in our hands, were not observed to ingest yeast bioparticles, microspheres or liposomes. Since both yeast cells and liposomes ranged in diameter between 10 and 15 μm, the lack of ingestion of these particles could indicate that engulfment is size dependent in the sinus/lacunae/vessel phagocyte population. However, size alone cannot explain these observations, since carboxylated microspheres were 1 μm in diameter. The differences in substrate specificity observed in both phagocyte populations suggest either a different hematopoietic origin or a common origin from the same precursor cell coupled with a microenvironment-dependent, specialization in function. Ballarin and colleagues have provided evidence suggesting that the phagocytic cells expressed in *B. schlosseri* colonies, namely, the macrophage-like cells and hyaline amebocytes, represent different functional stages of the same cell type (Ballarin et al., 1993; Ballarin and Cima, 2005). Specifically, under light microscopic observations, the hyaline amebocytes

Please cite this article as: Lauzon, R.J., et al., Phagocyte dynamics in a highly regenerative urochordate: Insights into development and host defense. Dev. Biol. (2012), http://dx.doi.org/10.1016/j.ydbio.2012.11.006

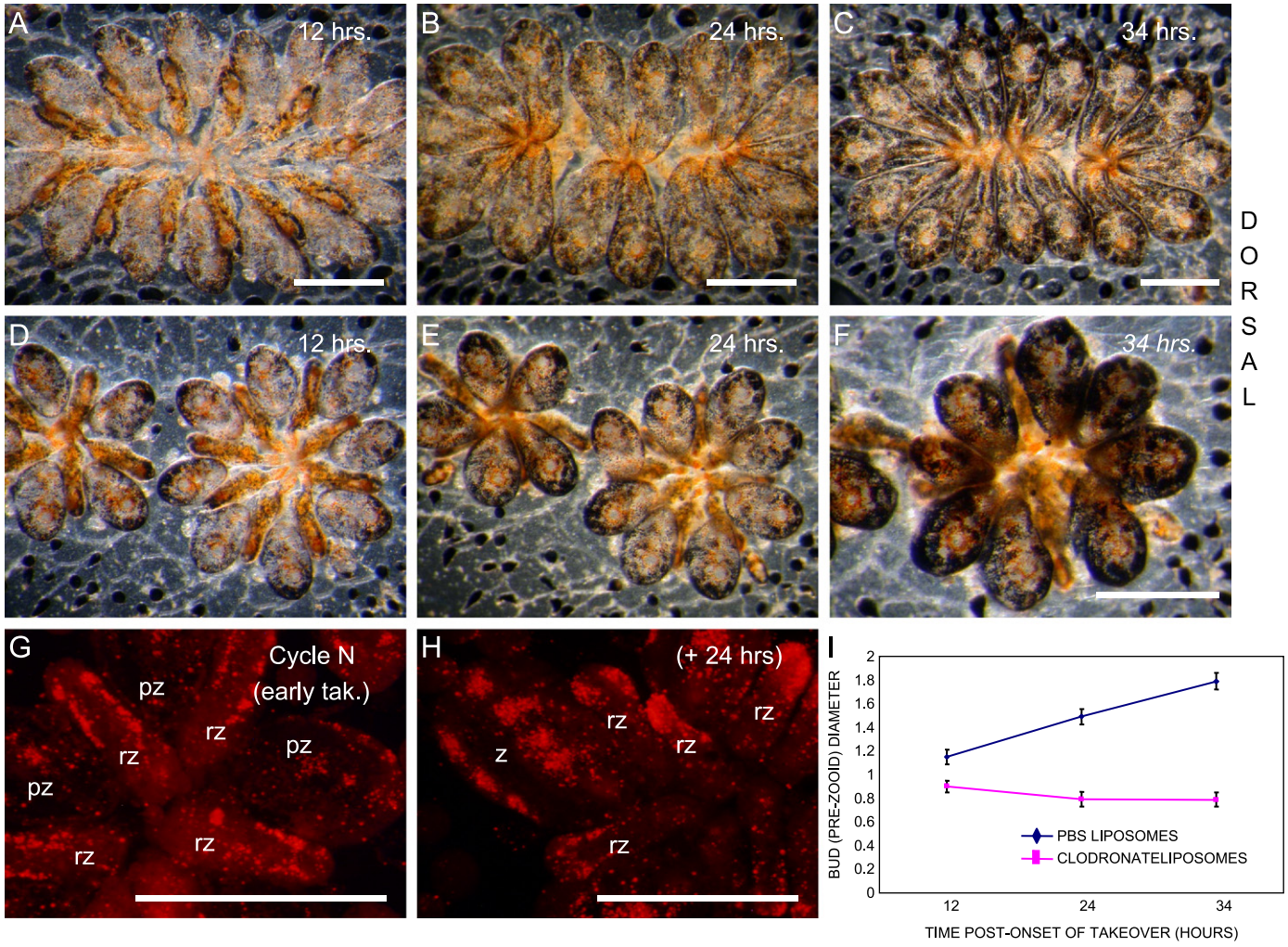

Fig. 10. Clodronate liposomes curtail zooid resorption during takeover. Single system, clonal replicate colonies were microinjected at stage 9/7/1 of cycle *N* with BODIPY-red PBS liposomes ((A)–(C)) and BODIPY-red clodronate liposomes ((D)–(F) and (G)–(H)), respectively. The colonies were subsequently observed during the progression of the takeover phase of the same blastogenetic cycle ((A)–(F)). Adult zooids are completely resorbed in the PBS liposome control, whereas zooid resorption is arrested in the clodronate liposome-microinjected clonal replicate. The pre-functional zooids from the clodronate-treated colony reach functional maturity, albeit with a reduced size when compared to the PBS liposome control (I). (G) Colony observed twenty-four hours following onset of takeover: many VIP are atypically still observed within the ventral islands of regressing adult zooids. Some VIP have homed and localized within ventral islands of pre-functional zooids. (H) Colony observed 24 h later during blastogenetic cycle *N*/*N*+1. Zooid resorption is curtailed and VI phagocytes still form discrete aggregates within the ventral islands of the unresorbed zooids. In contrast, mobile phagocytes have localized within discrete ventral islands in the functional generation of adult zooids. (I) Quantitative analysis of primary bud growth (pre-functional zooids) in PBS liposome- and clodronate liposome-microinjected, clonal replicates from the same colony as above. Note that bud (pre-zooid) diameter is significantly smaller in the clodronate-injected colony. Scale bars: 1 mm.

were found to exhibit an ameboid shape and were active in phagocytosis, whereas the macrophage-like cells were round and their cytoplasm contained multiple vacuoles filled with engulfed material (Ballarin et al., 1994). The mobile VIP are most likely the macrophage-like cells (discussed in the next paragraph), but it is unclear from our findings, whether the fixed phagocytes represent the hyaline amebocytes or a newly described phagocyte population. Whether indicative of a common precursor cell or not, characterization of phagocyte-specific, cell surface and/or molecular markers will be needed in order to distinguish between these two possibilities.

Ventral islands are sites of phagocyte turnover

The vascular parabiosis experiments allowed us to follow the behavior of the VIP population in real-time. In conjunction with ultrastructural observations, our findings strongly suggest that VIP circulate extensively throughout the colonial vasculature and maintain their functional state throughout blastogenesis. Their ultrastructural characteristics strongly suggest that they most likely represent the macrophage-like cells previously described (Burighel and Schiavinato, 1984; Lauzon et al., 1993; Ballarin et al., 1994). In our study, VIP were large cells that contained multiple phagolysosomes, indicative of phagocytic activity. Moreover, the VIP exhibited morphological changes indicative of cellular damage, which presumably led to their engulfment by neighboring VIP. These findings are consistent with those of Cima et al. (2010), in which they observed that senescent phagocytes were efficiently recognized and ingested by other phagocytes in the colony. They proposed that oxidative stress induced in response to prolonged respiratory burst could act as an underlying trigger responsible for phagocyte death and turnover. It is well documented that the macrophage-like phagocytes invade the regressing adult zooids during takeover, and these cells display extensive phagocytic potential, often engulfing multiple cell corpses (Burighel and Schiavinato, 1984; Lauzon et al., 1993; Ballarin et al., 1994). Given the massive tissue turnover, oxidative stress could be an important factor underlying the observations

Please cite this article as: Lauzon, R.J., et al., Phagocyte dynamics in a highly regenerative urochordate: Insights into development and host defense. Dev. Biol. (2012), http://dx.doi.org/10.1016/j.ydbio.2012.11.006

Table 1
Summary of liposome microinjections.

Characteristics of cyclic blastogenesis	% (*N*) of Colonies with curtailed or abnormal Blastogenesis								
	Non-injected Controls (*N*=10)	PBS Liposomes (microinjected in various stages) (*N*=29)				Clodronate liposomes (microinjected in various stages (*N*=36)			
		9/7/1 & 9/7/1+ (6)	9/8/2 & 9/8/3 (11)	9/8/4 & 9/8/5 (8)	Tak.(4)*	9/7/1 & 9/7/1+ (10)	9/8/2 & 9/8/3 (13)	9/8/4 & 9/8/5 (6)	Tak. (7)*
Zooid contraction[a]	100	100	100	100	100	100	100	100	100
Closure of siphons[a]	100	100	100	100	100	100	100	100	100
Loss of responsiveness to mechanical stimulus[a]	100	100	100	100	100	100	100	100	100
Curtailed zooid resorption[a]	0	0	9 (1)	12.5 (1)	0	80.0 (8)	100 (11)	80 (4)	100 (7)
Impaired blood flow/heart rate in regressing zooids[a]	0	0	9 (1)	14.3 (1)	0	20.0 (2)	15.4 (2)	0	14.3 (1)
Ampullar constriction/ Retraction	0	0	0	25.0 (2)	0	40.0 (4)	38.5 (5)	50 (3)	57.1 (4)
impaired growth of pre-functional zooids	0	16.7 (1)	0	0	0	50.0 (5)	53.9 (7)	83.3 (5)	71.4 (5)
Delay in secondary bud development	0	0	9 (1)	0	0	70.0 (7)	53.9 (7)	83.3 (5)	57.1 (4)
Increased VI cellularity and/or VI fusion	0	0	0	0	0	80.0 (8)	92.3 (12)	100 (6)	100 (7)
Loss of colony viability (colony death)	0	0	0	0	0	0	0	0	14.3 (1)

* Takeover.
[a] Takeover-specific events.

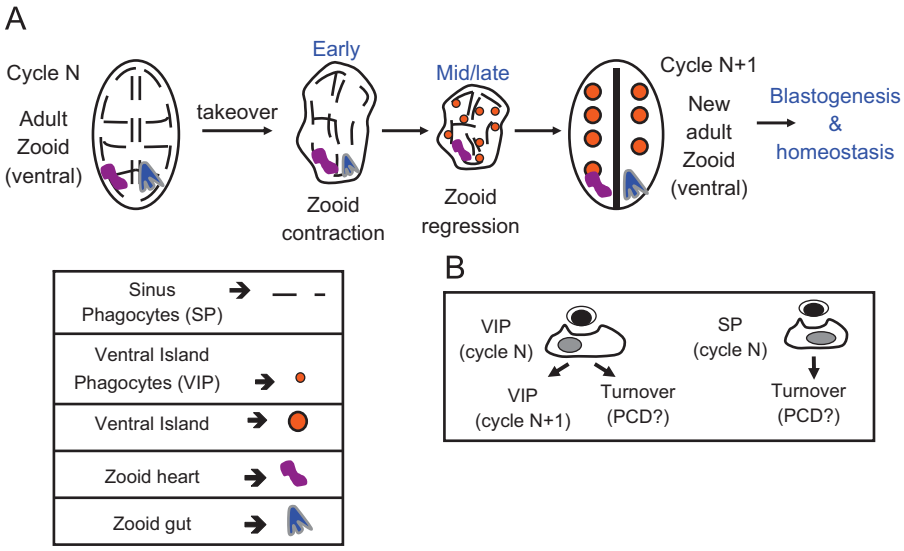

Fig. 11. A model for phagocyte homing and recirculation in *B. schlosseri*. (A) Two phagocyte populations are involved in colony homeostasis during each round of cyclic blastogenesis: ventral island phagocytes (VIP) and sinus/lacunae phagocytes (SP). VIP are mobile cells that recirculate extensively in the colonial vasculature, and home to zooid ventral islands at the beginning of a new blastogenetic cycle. Ventral islands exhibit a bilateral distribution along the zooid's antero-posterior axis. We postulate that, during the takeover phase of blastogenesis, VIP are involved in cell corpse engulfment and programmed cell clearance of the tissues and organs of the old zooid generation. In contrast, sinus/lacunae phagocytes are non-mobile (static) cells that line the sinuses and lacunae throughout the dorso-ventral axis adult zooids. These fixed cells are retained within the regressing zooid throughout takeover, and most likely turnover with each round of cyclic blastogenesis. Their specific role in zooid death and resorption is currently unknown. (B) Damaged or effete VIP turnover with each new round of blastogenesis: they undergo programmed cell death (PCD), are engulfed (programmed cell clearance) and replaced by newly-born phagocytes during a new blastogenetic cycle (turnover). Some of the "old" phagocytes may also survive and remain functional VIP in the new blastogenetic cycle. PCD: programmed cell death; SP: sinus phagocytes; VIP: ventral island phagocytes.

reported in our current study, as the majority of VIP appear to be phagocytosed within one cycle. In our vascular parabionts, co-localization of Alexafluor-green and -red fluorescence was observed in the same VIP. This suggests one of two possibilities: either a new phagocyte (born after microinjection was carried out, and thus unlabeled) randomly ate both a red and a green fluorescently labeled phagocyte or, an "old" (previously labeled) phagocyte of one color ate another "old" phagocyte of a different color. According to this model, damaged or effete phagocytes could either be cleared by newly born phagocytes that also exhibit homing properties to the VIs, or by other competing VIP (Fig. 11). At present, our current findings do not enable us to distinguish between these two possibilities, and whether VIP lifespan extends beyond a single blastogenetic generation. It is possible that some of the "old" phagocytes survive within the new zooid VI and remain as functional VIP in the new blastogenetic cycle (Fig. 11). An answer to this question will likely require their quantification by analytical flow cytometry using

Please cite this article as: Lauzon, R.J., et al., Phagocyte dynamics in a highly regenerative urochordate: Insights into development and host defense. Dev. Biol. (2012), http://dx.doi.org/10.1016/j.ydbio.2012.11.006

fluorescently labeled phagocytes from vascular parabionts. Nevertheless, the VIs likely represent niches where mobile phagocytes gather and undergo quality control and turnover in the new adult zooid generation.

Conversely, the fate of the static vessel phagocytes which line the sinuses and lacunae, and wall of the extracorporeal vasculature remains unknown. Using confocal imaging, we have demonstrated that these cells are retained within the regressing zooid throughout takeover, and most likely turnover with each round of cyclic blastogenesis. This conclusion is also supported in our vascular parabiont experiments. As expected, only the mobile, labeled VIP migrated in the ventral islands of the reciprocal fusion partner. The static, sinus/lacunae and vessel phagocytes remained in the original fusion partner. Significantly, labeled sinus/lacunae phagocytes were no longer visible within two generations (blastogenetic cycle $N+2$) following bioparticle microinjection. These observations are consistent with the idea that during cycle N (when microinjection is carried out), sinus/lacunae phagocytes from both adult zooids and developing primary buds ingested the fluorescent label. In contrast, secondary buds, which lack well developed sinuses would not be expected to harbor phagocytes and incorporate the fluorescent bioparticle label. One would therefore predict that regressing adult zooids during the takeover phase of both cycles N and $N+1$ would contain fluorescently labeled sinus/lacunae phagocytes, but not adult zooids during cycle $N+2$, as observed in this study.

Our ultrastructural observations further revealed that engulfment of damaged VIP by other phagocytes involved a collaborative, "tag-team" strategy. These cells displayed extensive pseudopodia as reported in this study, and some VIP were multinucleate (Lauzon, unpublished observations). The origin and identity of these cells is unknown at present, but may represent the hyaline amebocytes described by Ballarin et al. (1994). Regardless of their identity, our findings are consistent with the notion that quality control and turnover in the mobile, VIP population may involve a cellular fusion mechanism, analogous to that described for mammalian macrophages (Vignery, 2005). For instance, macrophage fusion in bone is essential in the formation of osteoclasts, which are critical effectors of bone resorption (Helming and Gordon, 2009). In addition, macrophage multinucleation is involved in the differentiation of giant cells, which are the hallmarks of granulomas found in chronic inflammatory states (Vignery, 2005; Helming and Gordon, 2009). In *Botryllus*, fusion of the macrophage-like cells found within VI may streamline the quality control process to ensure proper VIP homeostasis. Ingested VIP also displayed morphological changes characteristic of apoptosis, including cell condensation and margination of chromatin against the nuclear envelope. Tiozzo et al. (2006) used TUNEL (Terminal Deoxynucleotidyl transferase Nick End Labeling) to demonstrate that apoptosis occurred throughout blastogenesis in the developing buds and most prominently, in the regressing zooids during takeover. Our results strongly suggest that some of the TUNEL positive cells observed by Tiozzo et al. (2006) during takeover are the mobile VIP. In future studies, the use of the TUNEL assay in conjunction with ultrastructural studies of VIs carried out at various phases of blastogenesis may provide a more comprehensive approach to address this question more specifically.

Role of phagocytes in cyclical body regeneration and host defense

Our data is consistent with a model in which both phagocyte populations play a functional role in colony homeostasis and remodeling during each round of cyclic blastogenesis (Fig. 11). Since VIP are mobile cells that circulate extensively between VI and the colonial vasculature, we propose that, during the takeover phase, VIP are the principal cell population involved in cell corpse engulfment and programmed cell clearance of the tissues and organs of the dying zooid generation. This is supported by the observation that clodronate liposome microinjection, which selectively targeted and blocked VIP phagocytosis, also impaired zooid resorption and asexual reproduction. Interestingly, VIP were atypically observed within the ventral islands of unresorbed zooids from clodronate colonies. In contrast, VIP from control colonies microinjected with PBS liposomes or Alexafluor bioparticles had dispersed in the colonial vasculature by stage 9/8/5 of blastogenesis, and VI were not visible in the regressing zooids during takeover. These findings suggest that clodronate inhibits VIP mobility, and lends support to the hypothesis that VIP recirculation from the "old" blastogenetic generation to the "new" one is functionally involved in whole-body regeneration. Previous studies demonstrated that the presence of developing buds was not required to trigger the degeneration of the adult zooids but was essential to complete their resorption (Lauzon et al., 2002). A model was proposed in which circulating phagocytes function as trophic cells that deliver nutrients and/or growth maintenance factors to developing buds, which in turn, enables reconstitution of new bodies on a weekly basis (Lauzon et al., 2002, 2007). The findings presented in this study are consistent with this model. Furthermore, we have shown that budectomy did not affect of the dynamics of mobile phagocytes and their recirculation within the colony at different phases of blastogenesis. However, during takeover, VI were not observed in any of the colonies subjected to complete budectomy, and mobile phagocytes were scattered throughout the vasculature. In hemi-budectomized colonies, whereby a single primary bud was allowed to reach functional maturity, VIP homing was rescued and supernumerary sites were also observed. Lauzon et al. (2002) have previously shown that when the single remaining bud in a hemi-budectomized colony was allowed to reach functional maturity, it increased in size via hyperplasia, ultimately exceeding the dimensions of control, adult zooids (Lauzon et al., 2002). The findings presented here are in agreement with this latter study: we observed that these single buds ultimately developed into "superzooids" that expressed additional VI along the anteroposterior axis as well as supernumerary sites. Together, these findings are consistent with a model whereby successful trafficking of mobile phagocytes to VI is dependent on the expression of mesenchymal homing sites localized along the ventral surface of pre-functional and adult zooids. The presence of supernumerary VI are most likely indicative of the growth plasticity characteristic of this colonial animal (Sabbadin, 1994).

Sinus/lacunae and vessel phagocytes were never observed to ingest clodronate liposomes. Therefore it is unlikely that this cell population was directly affected by the treatment. Despite this, and the observation that these cells remained fixed in the regressing adult zooids throughout takeover, we cannot rule out their involvement in zooid resorption. Our experiments did not specifically address the role of either phagocyte population in host resistance against pathogens. Nonetheless, the observations reported in this study clearly indicate that both VIP and vessel phagocytes are endowed with the capacity to recognize, ingest and presumably break down Gram positive and Gram negative bacteria. We have recently shown that several Toll-like receptor genes are expressed and modulated throughout cyclic blastogenesis in *B. schlosseri* colonies (Lauzon, unpublished observations). Collectively, these findings support the notion that phagocytic cells of botryllid ascidians express functional pattern recognition receptors.

Hirose (2009) has previously documented that phagocytes are also present in the extravascular tunic of many colonial ascidians, including botryllids. We have also confirmed by transmission electron microscopy, that the tunic in *B. schlosseri* colonies contain significant numbers of phagocytes as well as morula cells (Lauzon, unpublished observations), a finding that is consistent with previously published observations (Zaniolo, 1981). However,

Please cite this article as: Lauzon, R.J., et al., Phagocyte dynamics in a highly regenerative urochordate: Insights into development and host defense. Dev. Biol. (2012), http://dx.doi.org/10.1016/j.ydbio.2012.11.006

accumulation of fluorescently labeled phagocytes in the tunic was never observed over several blastogenetic cycles following microinjection with Alexafluor bioparticles. Thus, as for the other two phagocytes populations described in our study, the hematopoietic origin of tunic phagocytes remains unclear. Our findings suggest one of two possibilities: tunic phagocytes may arise from precursors in the multipotent vascular epithelium, possibly through a de- or trans-differentiation mechanism similar to that reported in the polystyelid ascidian *Polyandrocara misakiensis* (Kawamura et al., 2008), or during whole body regeneration from isolated blood vessel fragments in *Botrylloides* sp. (Rinkevich et al., 1995; Brown et al., 2009; Rinkevich et al., 2010). Alternatively, engulfment of fluorescent bioparticles may curtail trans-endothelial migration of mobile and static phagocyte populations from blood to extravascular tunic.

Conclusions

In summary, we have demonstrated that botryllid ascidians are composed of distinct, mobile and static populations of phagocytes that are involved in organismal homeostasis. At present, it remains unclear what the hematopoietic origins of these cell populations are, and how each cell population impacts the other. The use of distinct phagocyte populations working cooperatively makes sense intuitively. Mammals, for instance utilize both neutrophils and macrophages, as a strategy to successfully target and eliminate dangerous microbes (Silva, 2010). On the other hand, the in vivo behavior and function of different types of phagocytes during tissue and organ regeneration is not yet characterized (Li et al., 2012). Collectively, the findings of this study are consistent with the notion that at least, the VIP play an instrumental role in homeostatic events that maximize the likelihood of increased colony survival and reproductive fitness. The weekly phases of blastogenesis and takeover, the experimental tractability of phagocytes and the phylogenetic position of *B. schlosseri*, and colonial ascidians in general, provide a unique model to investigate the functional link between programed cell death/clearance and organismal regeneration, and the roles that phagocytic cell populations play in colony survival, regeneration and host defense.

Acknowledgements

The authors would like to acknowledge the staff and facilities of the Marine Biological Laboratory, where the bulk of this work was carried out between the summers of 2004–2009. We would also like to thank Federico Brown and Anthony De Tomaso for critical review of this manuscript. The work was supported by a faculty research grant (Union College), a Laura and Arthur Colwin Endowed Summer Research Fellowship (RJL), and a Nikon Fellowship (ST).

Appendix A. Supplementary Information

Supplementary data associated with this article can be found in the online version at http://dx.doi.org/10.1016/j.ydbio.2012.11.006.

References

Ballarin, L., Cima, F., Sabbadin, A., 1993. Histoenzymatic staining and characterization of the colonial ascidian *Botryllus schlosseri* hemocytes. Ital. J. Zool. 60, 19–24.

Ballarin, L., Cima, F., Sabbadin, A., 1994. Phagocytosis in he colonial ascidian *Botryllus schlosseri*. Dev. Comp. Immunol. 18, 467–481.

Ballarin, L., Cima, F., 2005. Cytochemical properties of *Botryllus schlosseri* haemocytes: indications for morpho-functional characterization. Eur. J. Histochem. 49, 255–264.

Ballarin, L., Burighel, P., Cima, F., 2008. A tale of death and life: natural apoptosis in the colonial ascidian *Botryllus schlosseri* (urochordata: Ascidiacea). Curr. Pharm. Des. 14, 138–147.

Berrill, N.J., 1941. The development of the bud in Botryllus. Biol. Bull. 80, 169–184.

Bradford, M.M., 1976. A rapid and sensitive method for the quantification of microgram quantities of protein utilizing the principle of protein-dye binding. Anal. Biochem. 72, 248–254.

Brown, F.D., Keeling, E.L., Le, A.D., Swalla, B.J., 2009. Whole body regeneration in a colonial ascidian, Botrylloides violaceus. J. Exp. Zool. 312B, 885–900.

Burighel, P., Brunetti, R., 1971. The circulatory system in the blastozooid of the colonial ascidian *Botryllus schlosseri* (Pallas). Boll. Zool. 38, 273–289.

Burighel, P., Schiavinato, A., 1984. Degenerative regression of the digestive tract in the colonial ascidian *Botryllus schlosseri* (Pallas). Cell Tissue Res. 235, 309–318.

Burighel, P., Cloney, R.A., 1997. Urochordata: Ascidiacea. In: Harrison, F.W., Ruppert, E.E. (Eds.), Microscopic Anatomy of Invertebrates, 15. Wiley-Liss Inc., Hoboken, pp. 2211–2347, Hemichordata, Chaetognatha, and the invertebrate chordates.

Chang, Z.-L., 2009. Recent development of the mononuclear phagocyte 41system: in memory of Metchnikoff and Erlich on the 100th anniversary of the 1908 Nobel Prize in Physiology or Medicine. Biol. Cell 101, 709–721.

Cima, F., Manni, L., Basso, G., Fortunato, E., Accordi, B., Schiavon, F., Ballarin, L., 2010. Hovering between death and life: natural apoptosis and phagocytes in the blastogenetic cycle of the colonial ascidian *Botryllus schlosseri*. Dev. Comp. Immunol. 34, 272–285.

De Tomaso, A.W., Nyholm, S.V., Palmeri, K.J., Ishizuka, K.J., Ludington, W.B., Mitchel, K., Weissman, I.L., 2005. Isolation and characterization of a protochordate histocompatibility locus. Nature 438, 454–459.

Delves, P.J., Martin, S.J., Burton, D.R., Roit, I.M., 2006. Roitt's Essential Immunology. Blackwell, Oxford.

Elliot, M.R., Ravichandran, K.S., 2010. Clearance of apoptotic cells: implications in health and disease. J. Cell Biol. 189, 1059–1070.

Erwig, L.-P., Henson, P.M., 2007. Immunological consequences of apoptotic cell phagocytosis. Am. J. Pathol. 171, 2–8.

Fadeel, B., 2003. Programmed cell clearance. Cell. Mol. Life Sci. 60, 2575–2585.

Fadeel, B., Xue, D., Kagan, V., 2010. Programmed cell clearance: molecular regulation of the elimination of apoptotic cell corpses and its role in the resolution of inflammation. Biochem. Biophys. Res. Commun. 396, 7–10.

Helming, L., Gordon, S., 2009. Molecular mediators of macrophage fusion. Tr. Cell Biol. 19, 514–522.

Henson, P.M., Bratton, D.L., Fadok, V.A., 2001. Apoptotic cell removal. Curr. Biol. 11, R795–R805.

Henson, P.M., Hume, D.A., 2006. Apoptotic cell removal in development and tissue homeostasis. Trends Immunol. 27, 244–250.

Hirose, E., 2009. Ascidian tunic cells: morphology and functional diversity of free cells outside the epidermis. Inv. Biol. 128, 83–96.

Hume, D.A., 2006. The mononuclear phagocyte system. Curr. Op. Immun. 18, 49–53.

Izzard, C.S., 1973. Development of polarity and bilateral asymmetry in the palleal bud of *Botryllus schlosseri*. J. Morphol. 139, 1–26.

Jacobson, M.D., Weil, M., Raff, M.C., 1997. Programmed cell death in animal development. Cell 88, 347–354.

Kawamura, K., Sugino, Y., Sunanaga, T., Fujiwara, S., 2008. Multipotent epithelial cells in the process of regeneration and asexual reproduction in colonial tunicates. Dev. Growth Differ. 5, 1–11.

Kinchen, J.M., Ravichandran, K.S., 2007. Journey to the grave: signaling events regulating removal of apoptotic cells. J. Cell Sci. 120, 2143–2149.

Kinchen, J.M., Ravichandran, K.S., 2010. Identification of two evolutionarily conserved genes regulating processing of engulfed apoptotic cells. Nature 464, 778–782.

Kürn, U., Rendulic, S., Tiozzo, S., Lauzon, R.J., 2011. Asexual propagation and regeneration in colonial ascidians. Biol. Bull. 221, 43–61.

Laird, D.J., Chang, W.-T., Weissman, I.L., Lauzon, R.J., 2005. Identification of a novel gene involved in asexual organogenesis in a budding ascidian *Botryllus schlosseri*. Dev. Dyn. 234, 997–1005.

Lauzon, R.J., Ishizuka, K.J., Weissman, I.L., 1992. A cyclical, developmentally-regulated death phenomenon in a colonial urochordate. Dev. Dyn. 194, 71–83.

Lauzon, R.J., Patton, C.W., Weissman, I.L., 1993. A morphological and immunohistochemical study of programmed cell death in *Botryllus schlosseri* (Tunicata, Ascidiacea). Cell Tissue Res. 272, 115–127.

Lauzon, R.J., Ishizuka, K.J., Weissman, I.L., 2002. Cyclical generation and degeneration of organs in a colonial urochordate involves crosstalk between old and new: a model for development and regeneration. Dev. Biol. 249, 333–348.

Lauzon, R.J., Kidder, S.J., Long, P., 2007. Suppression of programmed cell death regulates cyclical degeneration of organs in a colonial urochordate. Dev. Biol. 301, 92–105.

Lemaire, P., 2009. Unfolding a chordate developmental program, one cell at a time: Invariant cell lineages, short-range inductions and evolutionary plasticity in ascidians. Dev. Biol. 332, 48–60.

Lettre, G., Hengartner, M.O., 2006. Developmental cell biology: developmental apoptosis in *C. elegans*: a complex CEDnario. Nat. Rev. Mol. Cell Biol. 7, 97–108.

Li, L., Yan, B., Shi, Y.Q., Zhang, W.Q., Wen, Z.L., 2012. Live imaging reveals differing roles of macrophages and neutrophils during Zebrafish tail fin regeneration. J. Biol. Chem., 22573321, May 9. [Epub ahead of print] PubMed PMID.

Please cite this article as: Lauzon, R.J., et al., Phagocyte dynamics in a highly regenerative urochordate: Insights into development and host defense. Dev. Biol. (2012), http://dx.doi.org/10.1016/j.ydbio.2012.11.006

Manni, L., Zaniolo, G., Cima, F., Burighel, P., Ballarin, L., 2007. *Botryllus schlosseri*: a model ascidian for the study of asexual reproduction. Dev. Dyn. 236, 335–352.
Milkman, R., 1967. Genetic and developmental studies on *Botryllus schlosseri*. Biol. Bull. 132, 229–243.
Mukai, H., Sugimoto, K., Taneda, Y., 1978. Comparative studies on the circulatory system of the compound ascidians, *Botryllus. Botrylloides and Symplegma*. J. Morphol. 157, 49–78.
Nakanishi, Y., Nagaosa, K., Shiratsuchi, A., 2011. Phagocytic removal of cells that have become unwanted: implications for animal development and tissue homeostasis. Dev. Growth Differ. 53, 149–160.
Reddien, P.W., Horvitz, H.R., 2004. The engulfment process of programmed cell death in *Caenorhabditis elegans*. Ann. Rev. Cell Dev. Biol. 20, 193–221.
Rinkevich, B., Shlemberg, Z., Fishelson, L., 1995. Whole-body protochordate regeneration from totipotent blood cells. Proc. Nat. Acad. Sci. U.S.A. 92, 7695–7699.
Rinkevich, Y., Rosner, A., Rabinowitz, C., Lapidot, Z., Moiseeva, E., Rinkevich, B., 2010. Piwi positive cells that line the vasculature epithelium, underlie whole body regeneration in a basal chordate. Dev. Biol. 345, 94–104.
Sabbadin, A., 1955. Osservazioni sullo sviluppo, l'accrescimento e la riproduzione di *Botryllus schlosseri* (Pallas) in condizioni di laboratorio. Boll. Zool. 22, 243–263.
Sabbadin, A., 1956. Studio sperimentale della gemmazione in *Botryllus schlosseri* (Pallas) [Ascidiacea]. Rend. Accad. Naz. Lincei (Cl. Sci. FF.MM.NN.) 20, 379–385.
Sabbadin, A., 1969. The compound ascidian *Botryllus schlosseri* in the field and in the laboratory. Pubbl. Staz. Zool. Napoli (37), 62–72.
Sabbadin, A., 1979. Colonial structure and genetic patterns in ascidians. In: Larwood, G., Rosen, B.R. (Eds.), Biology and Systematics of Colonial Organisms. Academic Press, London and New York, pp. 433–444.
Sabbadin, A., 1994. Coloniality in ascidians and its adaptive value, with special reference to *Botryllus schlosseri*. Anim. Biol. 3, 157–163.
Saito, Y., Hirose, E., Watanabe, H., 1994. Allorecognition in compound ascidians. Int. J. Dev. Biol. 38, 237–247.
Schulze, C., Muñoz, L.E., Franz, S., Sarter, K., Chaurio, R.A., Gaipi, U.S., Hermann, M., 2008. Clearance deficiency-a potential link between infections and autoimmunity. Autoimmun. Rev. 8, 5–8.
Scofield, V.L., Schlumpberger, J.M., West, L.A., Weissman, I.L., 1982. Protochordate allorecognition is controlled by a MHC-like gene system. Nature 295, 499–502.
Silva, M.T., 2010. When two is better than one: macrophages and neutrophils work in concert in innate immunity as complementary and cooperative partners of a myeloid phagocyte system. J. Leuk. Biol. 87, 93–106.
Stuart, L.M., Ezekowitz, A.B., 2005. Phagocytosis: elegant complexity. Cell 22, 539–550.
Tauber, A.I., 2003. Metchnikoff and the phagocytosis theory. Nat. Rev. Mol. Cell Biol. 4, 897–901.
Tiozzo, S., Ballarin, L., Burighel, P., Zaniolo, G., 2006. Programmed cell death during vegetative development: apoptosis during the colonial life cycle of the ascidian *Botryllus schlosseri*. Tissue Cell 38, 193–201.
Tiozzo, S., Brown, F.D., De Tomaso, A.W., 2008a. Regeneration and stem cells in ascidians. In: Bosch, T.C.G. (Ed.), Stem cells: from Hydra to Man. Springer Science+Business Media B.V., New York, pp. 95–112.
Tiozzo, S., Voskoboynik, A., Brown, F.D., De Tomaso, A.W., 2008b. A conserved role of the VEGF pathway in angiogenesis of an ectodermally-derived vasculature. Dev. Biol. 315, 243–255.
Tiozzo, S., De Tomaso, A.W., 2009. Functional analysis of Pitx during asexual regeneration in a basal chordate. Evol. Dev. 11, 152–162.
van Rooijen, N., 1989. The liposome-mediated macrophage 'suicide' technique. J. Immunol. Meth. 124, 1–6.
van Rooijen, N., Sanders, A., 1994. Liposome mediated depletion of macrophages: mechanism of action, preparation of liposomes and applications. J. Immunol. Meth. 174, 83–93.
van Rooijen, N., van Kesteren-Hendrikx, E., 2003. "In vivo" depletion of macrophages by liposome-demiated "suicide". Meth. Enzymol. 373, 3–16.
Vignery, A., 2005. Macrophage fusion: the making of osteoclasts and giant cells. J. Exp. Med. 202, 337–340.
Voskoboynik, A., Rinkevich, B., Weiss, A., Moiseeva, E., Reznick, A.Z., 2004. Macrophage involvement for successful degeneration of apoptotic organs in the colonial urochordate *Botryllus schlosseri*. J. Exp. Biol. 207, 2409–2416.
Weissman, I.L., 2000. Stem cells: units of development, units of regeneration, and units in evolution. Cell 100, 157–168.
Zaniolo, G., 1981. Histology of the ascidian *Botryllus schlosseri* tunic: in particular, the test cells. Boll. Zool. 48, 169–178.

Please cite this article as: Lauzon, R.J., et al., Phagocyte dynamics in a highly regenerative urochordate: Insights into development and host defense. Dev. Biol. (2012), http://dx.doi.org/10.1016/j.ydbio.2012.11.006